UNIVERSITY OF CALIFORNIA SAN DIEGO

Spontaneous Neurogenic Electromyographic Activities in ALS G93A Rats, Potential Over-Excitatory Drive Leading to Alpha Motor Neuron Degeneration

A Thesis submitted in partial satisfaction of the requirements for the degree Master of Science

in

Biology

by

Peixi Chen

Committee in charge:

Professor Martin Marsala, Chair
Professor Nicholas C. Spitzer, Co-Chair
Professor Stefan Leutgeb

2018

The Thesis of Peixi Chen is approved, and is acceptable in quality and form for publication on microfilm and electronically:

_____

_____

Co-Chair

_____

Chair

University of California San Diego

2018

DEDICATION

Though this journey has embarked an unprecedented turn, it is ultimately rewarding. I would like to dedicate this to those who persisted with me until the very end. Special thanks to Mariana, who provided me with immense support and guidance as we work on this project. Next, I would like to thank my cousin, Zhiling, and my best friend, Maylin, in providing me with valuable insights in experimental methodologies, and motivating me to move forward in research despite any hardships that arise. Without a doubt, I would not be able to go as far without my parents' trusts put into whatever that I strive to achieve.

Lastly, I would like to thank my thesis committee members, Dr. Martin Marsala, Dr. Nicholas C. Spitzer, and Dr. Stefan Leutgeb for agreeing to serve on my committee and inspiring me to further myself in the field of neuroscience.

EPIGRAPH

"Most of the threats we face, come from the progress we've made in science and technology. We are not going to stop making progress, or reverse it, so we must recognize the dangers and control them. I'm an optimist, and I believe we can."

Stephen Hawking

TABLE OF CONTENTS

LIST OF FIGURES

ACKNOWLEDGEMENTS

I would like to acknowledge Professor Martin Marsala for his support as the chair of my committee, and his approval for me to work on this new and exciting project. I would also like to acknowledge Mariana, who pushed me to think beyond my self-established boundaries and limits. Next, I would like to acknowledge Silvia Marsala, who has always shown immense encouragement in this process. Lastly, I would like to acknowledge Alex, or Oleksandr, for carrying out all electrophysiological recordings and sharing his knowledge in interpreting the corresponding results. It is their support that helped me in such an immeasurable way.

Chapter 1, in full, is currently being prepared for submission for publication of the material. Bravo-Hernandez, Mariana; Chen, Peixi; Platoshyn, Oleksandr; Marsala, Silvia; Marsala, Martin. “Spontaneous Neurogenic Electromyographic Activities in ALS G93A Rats, Potential Over-Excitatory Drive Leading to Alpha Motor Neuron Degeneration”.

Chapter 2, in part, is currently being prepared for submission for publication of the material. Bravo-Hernandez, Mariana; Chen, Peixi; Platoshyn, Oleksandr; Marsala, Silvia; Marsala, Martin. “Spontaneous Neurogenic Electromyographic Activities in ALS G93A Rats, Potential Over-Excitatory Drive Leading to Alpha Motor Neuron Degeneration”.

Chapter 3, in part, is currently being prepared for submission for publication of the material. Bravo-Hernandez, Mariana; Chen, Peixi; Platoshyn, Oleksandr; Marsala, Silvia; Marsala, Martin. “Spontaneous Neurogenic Electromyographic Activities in ALS G93A Rats, Potential Over-Excitatory Drive Leading to Alpha Motor Neuron Degeneration”.

ABSTRACT OF THE THESIS

Spontaneous Neurogenic Electromyographic Activities in ALS G93A Rats, Potential Over-Excitatory Drive Leading to Alpha Motor Neuron Degeneration

by

Peixi Chen

Master of Science in Biology

University of California San Diego, 2018

Professor Martin Marsala, Chair
Professor Nicholas C. Spitzer, Co-Chair

Amyotrophic lateral sclerosis (ALS) is a fatal neurodegenerative disorder characterized by a progressive degeneration of alpha-motor neurons, which results in motor-ambulatory and respiratory dysfunction. One of the proposed mechanisms generally believed to play a critical role in initiating alpha-motor neuron degeneration, is the hyperexcitable drive mediated by glutamatergic receptors in excitatory synapses due to elevated synaptic glutamates. However, no direct elctrophysiologically-defined data are available, which would provide an objective evidence on how overactivation of these receptors could lead to motor neuron degeneration in ALS. Our current study demonstrates that in fully awake SOD1^{G93A} rats, there are profound and

spontaneous α-motoneuron-mediated electromyographic activities measured at the level of gastrocnemius muscle, which is absent in age-matched wild type rats. This activity is effectively suppressed by isoflurane, NGX424 (AMPA receptor antagonist) and baclofen (GABAB receptor agonist). These treatments have no suppressive effect of muscle denervation-induced muscle fibrillation. Immunofluorescence and western blot analyses of lumbar spinal cord in SOD^{G93A} rats showed sustained presence of AMPA receptors and a significant increase in spinal VGluT1/2expression during end-stage at the lumbar intermediate zone. These data suggest an active participation of AMPA receptors and VGluT1/2 in mediating glutamate release and binding in observed overactivation of interneurons and alpha motor neurons. Additionally, unilateral sciatic neurectomy reduced VGluT1 expression and thus, the decrease of the more downstream muscle fibrillation. Accordingly, therapeutics reducing excessive glutamate receptor-mediated overexcitation, such as inhibition of excitatory interneuron-mediated glutamate release, or potentiation of spinal neuronal inhibition, may be effective in modulating alpha motor neuron degeneration in ALS.

Introduction

Amyotrophic Lateral Sclerosis (ALS) is a progressive adult-onset neurodegenerative disease often characterized by rapid degeneration of alpha motor neurons, which leads to muscle denervation. ALS generally falls into two categories: familial (fALS) and sporadic ALS (sALS). Though only 5-10% of total cases of ALS are familial in origin, this category remains to be phenotypically and genetically heterogeneous [25], thus overlapping with some of the clinical features of sALS as well [44]. In such cases, it is key to begin looking into familial ALS models in terms of approaching this yet-to-be curable disease.

The neuropathology of all ALS cases is mainly associated with mislocalization or abnormal accumulation of misfolded, insoluble protein aggregates in the cytoplasm of affected motor neurons [1] [19] [30]. These proteins are not strictly disease-specific but rather, are common proteins carrying out abnormal cellular functionality; this ultimately causes a collapse of protein homeostasis [6]. For example, the two proteins which encompass a large proportion in development of both fALS and sALS are misfolded Cu/Zn superoxide dismutase (SOD1) and cytoplasmic inclusion of TAR DNA binding protein (TDP-43), respectively [44]. The role of SOD1 enzyme is to protect cells from reactive oxygen species toxicity by breaking down superoxide radicals, whereas TDP-43 proteins are responsible for multiple steps of protein production: transcription, alternative splicing, and more. Although the misfolded SOD1 species are increasingly identified in non-SOD1 fALS and sALS cases [1] [10], this mutated genotype seems to only associate with ALS development. Although TDP-43 is a pivotal component of cytoplasmic inclusions in many forms of ALS, ubiquitous aggregations of this protein are also found in a common pathological subtypes of frontotemporal dementia (FTD) [23] [28], Huntington's disease [32], Alzheimer's disease [8], and many others. Since TDP-43 abnormality is

not restricted to ALS development, it is important to focus on analyzing SOD1-related pathophysiology to track down causations of motor neuron death in ALS.

According to the revised El Escorial criteria for classifying and diagnosing ALS for human patients/clinical research subjects, electromyographic (EMG) recordings denoting neurogenic potentials, fibrillation potentials, positive sharp waves, and fasciculation potentials are important electrodiagnostic tools for detecting early electrical signal abnormalities in ALS disease [22]. In fact, since these abnormalities appear exclusively in human patients with neurological symptoms, but not in healthy subjects, muscle fibrillations are considered as one of the hallmarks of muscle denervation in ALS. As there are no current studies which recapitulate such clinical signs in ALS animal models, establishing an equivalent model to track and intervene disease development, and further explore causes to hyperexcitabilities leading to motor neuron denervation, our group began recording EMG activities in young (age = 60d) and awake wild type and $SOD1^{G93A}$ transgenic rats. We proposed that the toxicities within alpha motor neurons were contributed by peripheral pathways where sensorimotor information were relayed to the spinal cord via the primary afferents.

Similar to peripheral nerve injuries or neurectomies, where spontaneous activities arise at approximately 7 days after a nerve is damaged [20], the neurogenic EMG potentials recorded in ALS patients could potentially resemble these injury-induced electrical events. Under these circumstances, the thresholds for spontaneously active neurons most likely shift under resting membrane potential, especially in the case of sciatic nerve injuries, where thresholds for nociception tend to decrease [33]. Underlying mechanisms such as increased sodium channel densities proximal to the site of axotomy in primary afferents [9], increased mRNA levels for

sodium channels expressed in dorsal root ganglion (DRG) after axotomy [39], and increased Ca^{2+} channel buffering could all contribute to the emergence of spontaneous activities [42].

As motor neuron neurotoxicities are often exacerbated by excessive glutamates available at excitatory synapses, multiple intrinsic properties can augment neurotoxicity [37]. In fact, an elevated glutamate level could be a result of insufficient glutamate reuptake (after release) via EAAT/GLT-1 in the glial cell populations such as astrocytes [37], increased presynaptic expression of vesicular glutamate transporters leading to larger quanta of neurotransmitters released (our study), and increased postsynaptic membrane sensitivities to glutamate binding and thus elevated permeabilities to Ca^{2+} ions, particularly via the rise of expression level of α-amino-3-hydroxy-5-methyl-4-isoxazolepropionic acid receptor (also known as the AMPA receptor) and the N-methyl-D-aspartate receptor (NMDA receptor) [37]. The enhanced membrane hyperexcitability activates downstream cascades after ion influxes through postsynaptic receptors, in which enzymes such as proteases, endonucleases and phospholipases become activated to disrupt cellular structures [37].

In our study, we attempt to characterize a contribution of increased excitatory neuronal drive in neuronal degeneration of G93A rats. Moreover, we also try to define the potential role of primary afferents-evoked glutamate release and observe the variations in key receptor protein expressions that ultimately induce alpha motor neuron excitotoxicity and degeneration.

Chapter 1. Materials and Methods

Animals

All animal experiments were conducted according to the protocols approved by the Institutional Animal Care and Use Committees of University of California, San Diego. Efforts were made to minimize the number of animals used in our study. Both sexes of wild type (WT) and $SOD1^{G93A}$ transgenic (Tg) rats were studied, where the wild type rats were regarded as the age-matched controls for the Tg rats. The homozygous Tg male Sprague-Dawley (SD) rats were crossed with wild-type female SD rats to breed hemizygotes. Tail DNA of these transgenic progenies were genotyped via polymerase chain reaction to detect the exogenous human SOD1 transgene; primers used were described previously [27]. Throughout the experimental period, all rats were housed in a specific pathogen-free animal facility, where food and water were available ad lib.

Intrathecal Catheterization

Intrathecal catheterization was performed on WT (120 d) and Tg (110 d) rats ($n \geq 6$) using a previously reported method [43]. Animals were anesthetized with 3% isoflurane, after which were placed in a stereotaxic head holder. The atlantooccipital membrane was exposed and pierced for a polyethylene catheter (PE-10, 8 cm length) to be inserted into the cistern magna and moved toward the thoracolumbar region until the lumbar intrathecal space was reached. Rats were housed and allowed to recover for 5 days before drug administration and testing.

Intrathecal Drug Delivery and Data Collection

Since the external portion of the intrathecal catheter was attached to a hand-operated micro-injector through an opening on the side of the rat restrainer, intrathecal injection of 10 µL NGX 424 (10µg/rat) or Baclofen (1µg/rat) were administered followed by a 10 µL flush of

sterile saline; the catheter was resealed with stainless steel plug immediately after injection. NGX424 (Tezampanel, a competitive antagonist of the AMPA and kainate subtypes of the ionotropic glutamate receptor family) and Baclofen (a derivative of GABA) were both freshly dissolved in 0.9% sterile saline on the day of drug administration. Baseline spontaneous muscle activity was recorded using electromyography (EMG) in awake animals before, 30 minutes after, and 24 hours after drug delivery.

Sciatic Neurectomy

Presymptomatic WT and Tg rats (60d) received left sciatic neurectomy under 2.5% isoflurane anesthesia (n = 3 per group). A skin incision cutting through the connective tissue between the *gluteus superficialis* and *biceps femoris* muscles allowed the sciatic nerve to be exposed. Two silk ligatures were then applied around the sciatic nerve at a distance of 0.5 cm away from each other to arrest epineural blood flow, from which an approximate of 0.2cm segment of the sciatic nerve was removed using surgical scissors. The wound was later closed with sutures in the muscle and staples in the skin; animals were allowed to recover from surgery.

Assessments to Measure ALS Progression

Both WT and Tg animals were weighed weekly after 30 days of age with an electronic scale. Generally, a 10% reduction in weight was deemed as the measure of symptomatic onset of ALS for Tg animals [24]. All affected Tg animals, with the exception of catheterized animals, were tested weekly for the ability to right themselves when positioned supinely [11]. Failure to right themselves within 30 sec was determined to be the end-stage of disease [14].

Resting Electromyography (rEMG) Recording

WT and Tg rats were either awake or anesthetized by 2.5% isoflurane with both left and right hind limbs shaved. For electromyography (EMG) recording, two 30-gauge platinum

transcutaneous needle recording electrodes (Grass Technologies, Astro-Med) were inserted (roughly at 1cm apart) into the gastrocnemius muscle of these rats. They were connected to an active head-stage (3110W Headstage; Warner Instruments), which was connected to a DP-311 differential amplifier for signal amplification and relayed to digitalization by the PowerLab 8/30 data-acquisition system (ADInstruments). The recorded signal was sampled at 20kHz and stored in a computer for further analysis.

Time course of muscle fibrillation and the corresponding alpha-motoneuron degeneration were characterized with EMG every 3-4 days until animals reached 10% body weight loss (from peak weight). A subpopulation of animals was perfused with 4% paraformaldehyde (PFA) at different time points: a) first signs of fibrillation (1^{st} FIB), b) 1^{st} FIB + 7 days, c) 1^{st} FIB + 14 days and d) 10% body weight loss (BWL). These perfusion groups were designed to compare the total number of alpha motoneurons persisted in lumbar spinal segments.

Then, EMG activity was recorded in awake WT and Tg rats that received intrathecal catheterization. Baseline EMG was collected immediately before NGX424 or Baclofen was administered, followed by a recording done at 30 minutes after drug delivery. Later, EMG was taken when these animals were fully anesthetized with isofluorane. Finally, EMG recording was collected once again at 24 h after drug delivery in awake, behaving animals.

Animals with left sciatic neurectomy were recorded every week until they lost 10-20% body weight. These animals were then perfused with 4% PFA; VGluT1 expression level and alpha-motoneuron level in lumbar 1-5 spinal segments were later quantified by immunohistochemistry.

***In vivo* Dorsal Root Recordings**

Symptomatic WT and Tg rats (10-20% BWL) were anesthetized with 3% isoflurane; their core body temperature was maintained at 37 ºC with a heating blanket. Laminectomy allowed exposure of the segments between lumbar 3 (L3) and sacral 1 (S1) of the spinal cord. The dura mater of the spinal cord was then incised, providing a full exposure of the spinal cord; warm mineral oil was applied to this site. To prepare for dorsal root recording, the left L5 dorsal root was hooked with two silver ball recording electrodes to record spontaneous neurogenic activities. Two stimulating 30-G platinum needle electrodes (Grass Technologies, Astro-Med) were also placed transcutaneously, but transverse to the intraplantar muscle of the animal. The paws of the animals were then stimulated thrice at 2-minute intervals using a square pulse, with an intensity of 6 mA and duration of 0.5 ms to ensure maximal stimulation of the primary afferents. The recording electrodes were connected to an active head-stage (3110W Headstage; Warner Instruments), which was connected to a DP-311 differential amplifier for signal amplification, and relayed to digitalization by the PowerLab 8/30 data-acquisition system (ADInstruments). The recorded signal was sampled at 20kHz and stored in a computer for further analysis.

Western Blot

Animals were perfused with 0.9% cold saline, followed by a spinal cord harvest with the lumbar segment excised and placed in cold isotonic saline solution. This excised tissue was quickly placed inside a closed tube to be snapped frozen in liquid nitrogen for 1 minute, after which an extraction using the cold protein lysis buffer (0.2 % NP-40, 1.5x EDTA-free Mini cOmplete, 10mM PMSF and 0.02M β-mercaptoethanol in MiliQ water) and quantification using Bradford assay (Bio-Rad) were done. An equal amount of protein was separated by 10% SDS-PAGE gel (Life Technologies Corporation) electrophoresis and later transferred to

polyvinylidenedifluoride (PVDF) membranes. After the membranes were blocked with 5% skim milk in Tris-buffered Saline with 1% Tween for 1 h at 4 ºC, they were then incubated overnight at 4ºC with rabbit anti-GluR1 subunit-containing AMPA receptors (clone C3T, Cat #04-855; 1:5000, Milipore) or mouse anti-pan-AMPA receptors (GluR1-4, clone 2D8, Cat # MABN832; 1:2000, Milipore) in blocking solution. Then, these membranes were incubated in horseradish peroxidase-conjugated secondary antibody (1:2000, Life Technologies Corporation) for 1 h at 4 ºC. Protein signals were detected using an enhanced chemiluminescence detection system. Blots were then stripped and re-stained with monoclonal antibody against β-actin (clone GT5512, Cat # 629630; 1:5000, GeneTex); the ratio for the protein examined was normalized against β-actin expression.

Immunohistochemistry

Animals were euthanized with intraperitoneal injection of pentobarbital (100mg/kg), and transcardially perfused with cold, heparinized saline (roughly at 300mL) followed by the perfusion of 4% paraformaldehyde (roughly at 300mL) dissolved in 0.15M sodium phosphate buffer (pH 7.4) at a flow rate of 18-25 mL/min. The spinal cord was post-fixed overnight and cryoprotected for 72 h in 30% sucrose in 1X phosphate buffer solution. To discriminate the left and right side of the spinal cord, a tissue dye (Davison Marking system, Bradley products, Inc.) was applied to indicate the left side of the spinal cord. The lumbar spinal cord was embedded in Optimal Cutting Temperature matrix compound (Tissue-Tek; Sakura Finetek), frozen inside the cryostat at -25ºC and transversely sectioned into 30µm thick sections; they were later transferred into 6-well plates filled with 1X phosphate buffered saline (1X PBS) with 0.01% thimerosal added. These sections were washed 3 times using 1X PBS solution with 0.3% Triton X-100 added (1X PBS + 0.3% TX-100), followed by blocking with 5% normal donkey serum in 1X

PBS + 3% TX-100 for 1h. Lastly, these blocked sections were immunostained overnight at 4ºC with the following primary antibodies in blocking solution: chicken anti-NeuN (neuronal neuclei, Cat. # ABN91, 1:1000; Millipore), goat anti-ChAT (choline acetyltransferase, Cat # AB144P, 1:100; Millipore), rabbit anti-GluR1 (glutamate receptor 1, C3T clone, Cat # 04-855, 1:1000; Millipore), guinea pig anti-VGluT1(Cat# AB5905, 1:1500; Millipore), and guinea pig anti-VGluT2 (Cat # AB2251-I, 1:2000; Millipore). Sections were washed in 1X PBS + 0.3% TX-100 for 3 times and incubated in secondary antibodies conjugated to different fluorescent Alexa Fluor® dyes for 1h at room temperature. Finally, sections were washed, mounted on glass slides, treated with ProLong Gold Antifade Mountant with DAPI (Invitrogen), and covered by coverslips.

Microscopy

Fluorescence images were captured using a fluorescent microscope (Zeiss AxioImager M2 Microscope, Carl Zeiss) at consistent exposure settings using the 10X, 20X as well as 60X immersion objectives, along with the Stereo investigator software (MBF Bioscience). Mosaic images were captured either from the entire transverse region, or just the ventral horn region, of the spinal cord sections at optimal intensity and clarity, with ample spectral separation between independent fluorophore detection, to obtain a good focal plane. To distinguish between antigens immunostained with different fluorophores, ImageJ was utilized to separate and later, merge multi-channel images into a single-color composite image. Through the use of an apotome accessory tool, high magnification images were created in Z-stack of 30 optical sections with 0.3-0.5 µm steps. Identical settings were kept across all sections in multiple microscopy sessions. Complete Z-stack images were loaded into ImageJ where the Z-projections with average intensity were generated.

Alpha Motor Neuron Quantification

WT and Tg rats were used ($n \geq 3$) where their L1-5 spinal cord segments were (30 μm free-floating, transverse sections) sectioned, and stained with ChAT antibodies. Six sections (selected from every lumbar segment of each animal), each at approximately 230 μm apart from one another, were selected for motor neuron quantification through Zeiss microscope and ImageJ software. Only alpha motor neurons with normal morphology and visible nucleolus were counted. For Tg rats which received left sciatic neurectomy, the left and right sides of the spinal sections were analyzed independently.

Interneuron Quantification

Spinal sections from the L4 and L5 segments of WT and Tg rats at end stage ALS ($n \geq 3$) were stained with NeuN antibodies. Similar quantification methods were carried out as described in the alpha motor neuron section. Virtual tissue images of spinal intermediate zones were acquired using the Zeiss microscope and Stereo Investigator software. These images were then loaded onto ImageJ, where the "Analyze Particles" option was selected to look for interneuron at sizes of 60-100 μm^2 and a circularity of 0.0-1.0 within laminae I, II (dorsal horn), and VII (intermediate zone).

VGluT1 and VGluT2 Quantification

Spinal sections ($n \geq 3$) of WT and Tg rats (symptomatic and at end-stage) from Lumbar 1-5 segments were stained with VGluT1 and VGluT2 antibodies. Similar quantification steps as described in the alpha motor neuron quantification section were carried out. Virtual tissue images of spinal transverse sections were acquired; they were loaded onto ImageJ where their integrated signal density was measured and outputted: VGluT1 and VGluT2 of end-stage animals and

controls were measured in lamina VII. In contrast, Tg and WT rats which received left sciatic neurectomy had VGluT1 integrated density (on both left and right) quantified and analyzed independently throughout the grey matter.

Phospho c-Jun Quantification

Lumbar 4 and 5 spinal segments from WT rats and Tg rats (n ≥3 animals; pre-symptomatic, symptomatic or end stage) were stained with phosphor-c-Jun Ser73 antibody. Six sections per segment per animal with at least 230 μm spacing were selected for quantification. Virtual tissue images of whole transverse sections were acquired at 10X using a Zeiss microscope and Stereo Investigator software. C-Jun-positive images were loaded onto Image-Pro Premier, with a polygon structure selected to outline the grey matter; it defined the region within the boundary as desired location for signal detection. Smart segmentation was then selected to separate positive staining from background by using multi-parameter separation algorithm. It allowed quick selection of positively stained neurons as objects, and the remaining auto-fluorescing region as background. Since this classification was done primarily based on pixelation level, the mean values for both objects and background were calculated, prior to the program's automatic selection for signals of interest. It was noted that pixel intensity at mean or higher were detected as objects (signals); therefore, it was important to further filter this data in order to avoid inclusion of fluorescing crystal debris found on the spinal sections. Additionally, the measurement range was defined using three morphological parameters: area, circularity, and size count. These were selected solely to identify the specific ranges that were desired to better identify positive signals. Lastly, c-Jun-positive images were analyzed by automated counting of positively stained neurons. The settings for selection and counting (with an exception for polygon outline) were saved and later applied to the remaining c-Jun images.

Statistical Analyses

All data were plotted and analyzed using Graphpad Prism 5. Group differences in each assay at every time point were analyzed by the student's t-test or one/two-way ANOVA, followed by Bonferroni-adjusted t-test for each two-group (multiple) comparison.

Chapter 1, in full, is currently being prepared for submission for publication of the material. Bravo-Hernandez, Mariana; Chen, Peixi; Platoshyn, Oleksandr; Marsala, Silvia; Marsala, Martin. "Spontaneous Neurogenic Electromyographic Activities in ALS G93A Rats, Potential Over-Excitatory Drive Leading to Alpha Motor Neuron Degeneration".

Chapter 2. Results

Time-course Development of Muscle Fibrillations and their Corresponding Progressive Loss of α-Motor Neurons

As one of the electrodiagnostic hallmarks of ALS in human patients [2], muscle fibrillation detection via electromyography serves as an important tool for early disease monitoring. Though a previous study demonstrated the presence of muscle fibrillation in rat models with ALS-like phenotypes, detailed correlation of disease progression to muscle denervation and hence, the loss of alpha motor neuron, is still lacking [15]. Continuous monitoring of EMG activities in presymptomatic animals demonstrated that the first sign of fibrillations appeared at 105±11 days (Figs. 1B & 1D), which were on average 18 days prior to 10% body weight loss, which occurred at 123±14 days. Quantitative analysis showed 5-10% α-motor neuron loss when the first fibrillation event was detected (1st FIB), 35-40% loss at 1st FIB + 7 days, 60-70% loss at 1st FIB + 14 days, and approximately 80% loss at 10% BWL (Fig. 2A-B). These findings support the use of EMG measurement as a more accurate way to identify early neuronal loss in rats, as well as an indirect measurement of symptom onset.

Spontaneous Neurogenic EMG Activity in Awake Symptomatic SOD^{G93A} Rats was AMPA Receptor-dependent

Neurogenic spontaneous EMG activity, with the absence of peripheral stimulation and voluntary control, was recorded in the gastrocnemius muscle of awake, behaving symptomatic SOD^{G93A} rats of 110 d (Fig. 3A). This was then compared to the activities recorded after isoflurane induction, which blocked neuronal activity and hence, the neurogenic component of recorded EMG. An approximately 50% decrease in the spontaneous neurogenic EMG activity was recorded at 30 minutes after intrathecal administration of baclofen. More strikingly, 80% of

this activity was inhibited at 30 minutes after NGX424 was administered (Figs. 3B & 3E). Furthermore, induction of deep isoflurane anesthesia produced a near-complete block of the EMG activity in all symptomatic SOD1 rats; this administration unmasked fibrillation potentials, which were independent of spontaneous neurogenic activity and undisturbed by the anesthetics administered (Figs. 3C). The remaining uninhibited spontaneous neurogenic EMG activity could be due to over-activated NMDA receptor, as was shown *in vitro* previously [18]. Spinal spontaneous activities reappeared 24h post-administration of anesthetics, of which the effects had worn off (Figs. 3D & 3E).

Expression Modification of AMPA Receptors in the Spinal Cord during ALS progression

To verify that the binding sites for NGX424 were present for WT and Tg animals (from the 1st FIB cohort), GluR1 expression was confirmed. In fact, GluR1 immunostaining encompassed the entire grey matter: ventral horn (Fig 3F), dorsal horn (Fig. 4A), as well as the intermediate zone (Fig. 4B) of the spinal cord sections; progressive decrease in expression was observed from presymptomatic- to end-stage (Figs. 4C & D). Western blots indicated a trend of decrease in GluR1 expression; however, the reduction was insignificant. Protein expression of pan-AMPA receptor subunits (GluR 1-4) was also evaluated via immunohistochemistry. The expression levels of these receptor subunits remained relatively stable at presymptomatic stage, followed by rapid declines at end-stage (Fig. 4E). These observations aligned with persistent loss of alpha-motoneurons throughout disease advancement, which indicated that expressions of individual AMPA receptor subunits may have been rearranged (lost or gained) at first sign of muscle fibrillation, during which approximately 10% of the alpha motoneuron population degenerated (Fig. 2B). Previous studies also noted differential expression levels of AMPA subunits during ALS development in G93A mice [36].

Sustained Primary Afferents Inputs in Clinically Symptomatic and Wild Type Rats

To assess dorsal root activity as one of the potential causes of neurogenic spontaneous EMG activity, a peripheral electrical stimulus in both wild type and symptomatic rats with 10-20% BWL produced a corresponding recruitment of all peripheral axon fibers. The amplitude of the axonal response was not significantly different between Tg symptomatic (30.9 ± 4 mV) and wild type (33.2 ± 6 mV) animals (Fig. 5). This result suggested that all primary afferent nociceptors or thermoreceptors (types I and IIo/IIi) were intact and functional in symptomatic $SOD1^{G93A}$ animals. Therefore, peripheral inputs could be a possible contributor to excessive glutamate release, insufficient GABA release, or both, leading to the presence of the neurogenic spontaneous activity.

Alpha-motoneruon Survival after Unilateral Sciatic Neurectomy in Pre-symptomatic $SOD1^{G93A}$ Animals

To further pinpoint inputs at the level of primary afferents for inducing spontaneous neurogenic EMG activity and subsequent motoneuron death, the left sciatic nerve of Tg presymptomatic rats (60 d) and age-matched wild type rats were severed. EMG recording was carried out in both the left and right hind limbs of both groups every week; fibrillation potential was monitored until 10-20% BWL. Although these potentials appeared soon after the left hindlimb of both animal groups underwent sciatic neurectomy, fibrillation at the neurectomied side of Tg presymptomatic rats developed less intensely as compared to their uncut limb as ALS proceeded (Supplementary Fig. 1). All animals were later perfused, with their L1-5 spinal segments quantified. Wild type animals (Fig. 6A & B) did not show significant changes in alpha-motoneuron count when ventral spinal cord segments were analyzed through the comparison between the ipsilateral (cut site) and contralateral sides (Fig. 6C-F). Similarly, the alpha

motoneuron quantification in L1 and L2 segments of symptomatic rats (10% BWL) showed no difference in count when compared to wild type animals (Figs. 6B, D & F). Conversely, neurectomy in pre-symptomatic rats allowed significant motoneuron survival given the same comparison in L5 spinal segments (Figs. 6A & C), despite the unchanged alpha-motoneuron count detected in L4 segments (Fig. 6E), suggesting larger L5 contribution to the innervations of sciatic nerve.

VGluT1 Expression Increased in Wild Type and SOD1^{G93A} Rats after Sciatic Neurectomy

Presynaptic sensory or interneuronal levels of glutamate-containing vesicles (in the sensory-motor circuitry) were investigated for its role in alpha-motoneuron survival through VGluT1 expression quantification after sciatic neurectomy. Significant reduction in VGluT1 immunostaining in the L5 spinal segment were detected in the neurectomied side of both wild type and symptomatic animals (Figs. 7A & C) without visible changes in other segments (Figs. 7B & D-F). This corresponded with better alpha-motoneuron survival in symptomatic rats, as was shown in the previous section; however, sciatic neurectomy did not delay disease onset, nor did it slow progression in SOD^{G93A} rats.

VGluT1 and VGluT2 Expression and Spinal Interneuron Population at Lamina VII

While the population of interneurons was significantly reduced at the spinal intermediate zone in Tg symptomatic and end stage rats (Figs. 8A & B) when compared to wild type animals, immunodetection indicated that both VGluT1 and VGluT2 demonstrated significantly increased levels of immunoreactivity in the same region of end-stage animals (Figs. 8C-F). The elevated expression in excitatory synapses as ALS progressed may contribute to the imbalance in excitotoxic drive at late stage of disease development.

Induced Expression of Phosphorylated c-Jun at Serine 73 in Symptomatic and End-Stage Animals

Moreover, cell damages/deaths induced by oxidative stress was evaluated by assessing the activation of phosphorylated c-Jun (serine73) and its downstream effects, in addition to the time point it occurred during disease progression. Positive immunostaining of phospho-c-Jun in WT (Fig. 9A) or clinically pre-symptomatic Tg animals (Fig. 9B) were not detected; however, symptomatic and end-stage animals (Figs. 9C-D) demonstrated positive signals of nuclear phospho-c-Jun. These were primarily detected in the intermediate zone and the ventral horn of the spinal cord, co-localizing with NeuN immunostaining though not with GFAP (data not shown). Quantification confirmed intensification in expression of these phospho-c-jun positive neurons in rats with late-stage ALS (Fig. 9E).

Chapter 2, in part, is currently being prepared for submission for publication of the material. Bravo-Hernandez, Mariana; Chen, Peixi; Platoshyn, Oleksandr; Marsala, Silvia; Marsala, Martin. “Spontaneous Neurogenic Electromyographic Activities in ALS G93A Rats, Potential Over-Excitatory Drive Leading to Alpha Motor Neuron Degeneration”.

Chapter 3. Discussion

Early Identification of Motor Neuron Degeneration by Analyzing Fibrillation Potentials

While ALS progression has been thoroughly analyzed in SOD1^{G93A} rodents through parameters such as body weight loss, motor functions loss, biochemical and morphological changes [24, 27, 34], little was done to look at the electromyographic aspect of the disease progression in the same animal models [3].

In this study, we showed that EMG recording of fibrillation potentials is an effective electrodiagnostic method for measuring alpha motoneuron loss and identifying early disease symptoms in SOD1^{G93A} rats. It more precisely pinpointed the onset of motoneuron loss than 10% body weight loss, during which about 80% of motoneurons already degenerated. Additionally, retrospectively estimating the peak of body weight seemed less reliable in determining ALS onset, for that the disease may have already advanced with undesirable consequences. Similarly found in human patients, electrodiagnostic abnormalities denoted by the presence of fibrillation potentials in clinically defined normal muscles, are important diagnostic and prognostic features. They imply acute motoneuron denervation and rapidly progressive ALS, respectively [7]. It is valuable to have an equivalent disease model, which permits timely testing of therapeutics targeting clinically non-evident motor deficits, and simultaneously promote advancement in disease management before substantial sensory and motor deficits develop.

The Role of AMPA Receptors in Emergence of Spontaneous Neurogenic EMG Activities

Results showed that abnormal spontaneous neurogenic activities in the spinal cord, which were not found in age-matched wild type rats, appeared completely independent of muscle denervation demonstrated by fibrillation potentials. As intrathecal administration of drugs in awake and behaving animals (see methods) was carried out, a large reduction of spontaneous

neurogenic activities was observed as fibrillation potentials remains unchanged. In such cases, simultaneous administration of anesthetics along with EMG recording potentially masks important spinal circuitry, which could otherwise reveal neuronal activities leading to muscle denervation during ALS onset and progression. On the other hand, the said pharmacological intervention could also provide intriguing details regarding such spinal pathways, in which the increase in GABA-mediated inhibitory synapses and/or the decrease in glutamate-mediated excitatory synapses led to attenuation of spontaneous neurogenic activities. As was shown previously (see results), approximately 90% reduction in spontaneous activities was recorded when NGX424, an AMPAR antagonist, was intrathecally administered. Similarly, an activation of $GABA_B$ receptors through baclofen binding at the level of the lumbar spinal cord led to similar yet less effective reduction. Lastly, the administration of deep isoflurane (≥3%) enhanced release of GABA and sped up glutamate re-uptake (by decreasing the duration of excitatory transmission), which ultimately led to complete blockage of spontaneous activities. In all three drug deliveries, fibrillation potentials remain unchanged. From that, it is suggested that the alteration of neurotransmission styles at certain regions of the spinal cord plays a major role in inducing neurogenic spontaneous EMG activities. Furthermore, it is unlikely that these spinal activities directly trigger muscle denervation.

Next, protein expression of pan-AMPA receptor subunits (GluR1-4) was analyzed in time course animals, in addition to GluR1 subunit expression at the level of the spinal grey matter to investigate the specific changes in spinal circuitry. Interestingly, while the expression level of GluR1 subunit significantly declined in both presymptomatic and end stages, the level of all AMPA receptor subunits showed remarkable decline only at end-stage of disease (Fig. 4E). This is an indication that the expression level of individual AMPA receptor subunits vary during

disease progression. As explored by Virgo et al., in situ hybridization of post-mortem ALS human spinal homogenates revealed a significant 38% decrease in GluR A (GluR1) mRNA and 67% decrease in GluR B (GluR2) mRNA when compared to control tissue homogenates; mRNA levels of GluR3 and 4 were not considered as they were too low to be detected in human spinal tissues [38]. However, as the correlation between mRNA transcript levels and protein expressions is condition-dependent, high mRNA concentrations of AMPA receptor subunits do not necessarily dictate large protein abundance [21]. Therefore, it is crucial to assess protein concentrations in condition-specific manners. In fact, Tortarolo et al. demonstrated that GluR2 immunoreactivity was enhanced in the substantia gelatinosa of the lumbar dorsal horn at presymptomatic stage yet decreased at the ventral region during all disease stages in SOD^{G93A} mice [36]. Moreover, GluR3 immunoreactivity was shown to modestly increase during presymptomatic stage in lamina IX, whereas no change in GluR4 expression level was observed compared to age-matched controls [36]. Western blot analysis conducted by the same group further confirmed that ventral spinal homogenates from presymptomatic G93A mice had declined GluR2 protein expression when compared to non-transgenic control homogenates [36]. GluR2 is a key subunit of the AMPA receptor with biophysical properties including, but not limited to, receptor kinetics, single-channel conductance and Ca^{2+} permeability [17]. Specifically, AMPA receptors that lack GluR2 are said to be Ca^{2+} permeable, whereas those expressing GluR2 subunits have little to no Ca^{2+} permeability [17]. In this case, the diminishing trend observed in pan-AMPA receptors subunit (GluR1-4) expression over the course of disease development is mainly due to declining GluR2 subunit expression in the ventral lumbar region. This indirectly influences the excitatory neurotransmission of motor neurons in the ventral horn, where they were shown to be more susceptible to AMPA-mediated cytotoxicity than the dorsal

horn neurons [31]. These glutamatergic synapses become more likely to be preserved, if not hyperexcitable, as glutamate binding overactivates AMPA receptors and hence amplifies Ca^{2+} ion conductance. This induces a series of downstream amplification effects, which ultimately ends in excitotoxicity and thus large-scale motor neuron deaths [31]. In addition, it provides an explanation for the minimized excitatory neurotransmission as NGX424 competitively bound to the postsynaptic AMPA receptors; glutamate binding was made unlikely. By preventing subsequent Ca^{2+} influxes, this antagonist weakens the trigger for AMPA receptor activation and hence the downstream signaling cascades leading to motor neuron hyperexcitability and soon after, degeneration. Lastly, the remaining 10% of unsuppressed neurogenic spontaneous EMG activities might have been mediated by Ca^{2+} ion conductance via mostly NMDA receptors, which opened depending on AMPA receptor activation; rescue of functional NR1 subunit of the NMDA receptor demonstrated neuroprotection [31]. However, further identification of these channels is needed potentially via administration of competitive antagonist (such as R-2-amino-5-phosphonopentanoate, or APV) of NMDA receptors.

Input from Primary Afferents May Be a Source of Spinal Hyperexcitability that Drives Motor Neuron Degeneration

Besides intrinsic alteration of AMPA receptor subunit composition throughout ALS progression, external inputs, especially those implicated by synaptic glutamate concentration, onto motor neurons may further induce motor unit hyperexcitability and hence spontaneous firing at the skeletal muscle [37]. In this case, monosynaptic and polysynaptic sensory inputs from primary afferents, spinal interneurons, and the descending/ascending spinal tracts are essential sources of glutamate, the primary excitatory neurotransmitters found in the spinal cord circuitry.

To ensure that functions were intact in these regions, *in vivo* dorsal root recordings were carried out after evoked peripheral electrical stimulations; no significant amplitude changes in electrical responses were recorded in symptomatic rats compared to their WT counterparts. This suggests that conduction abnormality was not present at the level of primary afferents to impede synaptic neurotransmitter release. Furthermore, a decrease of ipsilateral VGluT1 immunostaining throughout the L5 segment after left sciatic neurectomy in presymptomatic animals indicated a generalized compromise in glutamate loading onto synaptic vesicles, as the source of VGluT1 transport had been disrupted. As discovered by Wojcik et al., the number of VGluT molecules per synaptic vesicle not only determined the neurotransmitter loading rate but also the quantal sizes, thus impacting the efficacy of neurotransmission [4, 40]. Given this information, a decrease in VGluT1 expression could lessen glutamate loading and quanta release from excitatory synapses of the primary afferents onto postsynpatic interneurons, glial cells and/or alpha motor neurons in the spinal cord, which ultimately led to a reduced likelihood of excitotoxicity-causing events. Indeed, the ipsilateral alpha motor neuron count and the corresponding fibrillation frequencies as a result of sciatic neurectomy resembled more closely to those detected in the WT lesion site, rather than the intact site in SOD^{G93A} animals. It was also speculated that the intact sciatic nerves of transgenic animals had elevating fibrillations recorded over time, similar to the condition observed in time-course $SOD1^{G93A}$ animals. This indicates that glutamate-dependent external inputs from the primary afferents contributed to alpha motor neuron survival and the more downstream muscle innervation during ALS progression.

In contrast, the alpha motor neuron count was unmodified in WT animals that also received neurectomy, even though apparent decreases in VGluT1 immunostaining were also observed on the ipsilateral side of the lesion site. Similarly, Hughs et al. observed progressive

reduction of VGluT1 immunostaining in laminae III, IV and especially IX (where VGluT1 staining is mostly located) in nontransgenic rats that underwent unilateral sciatic nerve transection [16]. In addition, the luminance value of VGluT1 detected per neuronal bouton (at central terminals of primary afferents) was detected to be lower in the lesioned side compared to the intact side [16]. Both cases demonstrated sharper reduction of VGluT1 levels at weeks after transection [16]. In fact, this was observed in the primary afferents of many WT rodents that underwent sciatic nerve transection, which were often used as models for peripheral nerve injuries. The ultrastructure of the spinal terminals of these models, including the dorsal and ventral horns, showed rather drastic reduction of glutamate concentration in synapses [5, 16]. Moreover, the emergence of spontaneous activities at the primary afferents is frequently detected soon after transection; they are typically accompanied by development of neuropathic pain in animal models [33, 41]. It is possible that those irregular action potential activities arise in both the WT and transgenic animals, particularly due to random membrane voltage fluctuations of the resting membrane potentials, or the lowering of action potential thresholds in dorsal root ganglion [33]. As for why alpha motor neurons are unaffected in WT rats, it is proposed that the possible causes of VGluT1 downregulation as a result of absence in excitatory inputs from primary afferents, account for motor neuron survival, but not development. Therefore, alpha motor neuron structure and count are not affected. Furthermore, the moderate glutamate deficiency in synapses may not be sufficient in inducing severe changes that would obstruct excitatory transmissions, thus allowing normal coordination within motor units to carry on. Although the causes of VGluT1 depletion remain to be elucidated, they are likely linked to the manifestation of spontaneous activities and disappearance of muscle fibrillation potentials due to nerve transection.

ALS disease onset and progression were not delayed nor prolonged albeit increased motor neuron count in the ventral spinal region ipsilateral to the lesion site. This indicates that the VGluT1 expression level is not necessarily a key determinant for motor neuron functionality and survival, but rather a byproduct of the main event that drives both motor neuron degeneration and muscle denervation.

It is noteworthy the limitation of this part of the experiment. The lack of EMG recording in both hindlimb gastrocnemius muscles and the injured nerves in awake, unilaterally transected transgenic and WT rats made it rather difficult to analyze the possible development and progression of neurogenic spontaneous activities, as well as pain-related behaviors in these animals. As a result, no direct correlation can be drawn from VGluT1 expression reduction to the possible production or the reduction of spontaneous activities at either the primary afferents or the muscle. Ideally, simultaneous bilateral measurements using EMG could demonstrate major differences in electrical activities, thus providing valuable insights regarding the origin of spontaneous activities and its relationship with motor neuron survival.

Contributions of Interneurons to Motor Neuron Stress

In this study, it is demonstrated that the interneuron populations in the spinal intermediate zone (laminae VII and X) were progressively and significantly reduced in SOD1^{G93A} rats, while the opposite is true for VGluT1 and VGluT2 expressions, starting at the symptomatic stage of ALS. Research findings from McGown et al. indicated that interneuron dysfunction predisposed motor neuron stress, which later showed hallmarks of ALS in zebrafish such as impaired motor function, motor neuron degeneration, disconnected neuromuscular junction, and muscle atrophy [26]. However, Hossaini et al. proposed an opposite pattern observed in ALS pathology, where the

loss of markers for inhibitory interneurons stemmed from motor neuron degeneration in $SOD1^{G93A}$ mice [13]. Although the overarching causation in neuronal death inside the spinal cord remain unclear, it is evident that the deaths of interneurons as well as motor neurons are linked.

As the neuronal activities inside the spinal cord are primarily dependent on the equilibrium between excitatory and inhibitory neurotransmission, which use glutamate and GABA (some glycine) as principal transmitters respectively, it is crucial to monitor the changes in these synapses as the disease progresses. In fact, it is expected that as the population of interneurons decrease, both inhibitory and excitatory transmissions would go down as a result. In a previous study, such was observed in inhibitory interneuron populations, where *in situ* hybridizations of lumbar GlyT2 mRNA (for glycinergic interneurons) and GAD67 mRNA (for GABAergic interneurons) in symptomatic mice tissues demonstrated a significant reduction in staining in both the intermediate zone and the ventral horn [13]. Immunofluorescence staining of GAD65-positive proteins done by our group indicated that the inhibitory dorsal horn interneurons were spared, as the level of immunostaining was not reduced in any disease development stages, and that the reduction in interneuronal count was not detected by NeuN staining (data not shown). This is possibly due to its lack of direct innervations or synaptic connections with alpha motor neurons, where impact of ventral motor neuron death is not retrospectively received by dorsal horn interneurons [35].

However, the excitatory neurotransmission did not seem to be impacted by the death of interneurons in the intermediate zone. Interestingly, vesicular glutamate transmitters, which control the quantal release of neurotransmitters in synapses, increased significantly during disease end-stage despite the loss of transmission media. It is predicted that elevated VGluT1 and VGluT2 protein expressions were primarily in surviving interneurons, which had not yet

succumbed to neuronal stress. In such cases, it is possible that this is an attempt of the spinal circuitry to maintain excitatory functionality through amplifying the transporter storage. Moreover, though unlikely, it may implicate acute cell damages, during which the neuronal contents break down and spill into the extracellular spaces of the spinal intermediate zone. It is pivotal to locate these cellular contents using techniques such as ex vivo imaging in order to observe whether this indeed was the result of programmed cell death.

Activation of Phosphorylated c-Jun Specifies Cell Deaths Induced by Oxidative Stress

Starting at the clinically symptomatic stage, $SOD1^{G93A}$ rats showed sharp increase in immunostaining of N-terminally phosphorylated c-Jun at its serine 73 residue, which tightly associated with acute cell damages and onset of apoptosis in adult rats [12]. Interestingly, the colocalizations of c-Jun with NeuN immunstaining detected in spinal segments from symptomatic animals are more evident than end-stage animals. This implicates that the reduction of staining overlap, where phosphorylated c-Jun activation could underlie neuronal hyperexcitability before cellular damages commence, is a sign of neuronal death which followed soon after motor dysfunctions arise. In addition, it further proves that the elevated expressions of vesicular glutamate transporters 1 and 2 (see previous section) could be the product of necrosis (traumatic cell death as a result of injuries), during which the membrane integrity of cells were lost, thus leading to cellular content spillage [29].

Chapter 3, in part, is currently being prepared for submission for publication of the material. Bravo-Hernandez, Mariana; Chen, Peixi; Platoshyn, Oleksandr; Marsala, Silvia; Marsala, Martin. “Spontaneous Neurogenic Electromyographic Activities in ALS G93A Rats, Potential Over-Excitatory Drive Leading to Alpha Motor Neuron Degeneration”.

Chapter 4. Conclusion

This is the first report tracking the development of abnormal spontaneous neurogenic activities using electromyographic recordings in awake and behaving symptomatic SOD1^{G93A} animals, where delivery of anesthetics via intrathecal catheterization attenuated AMPAR-mediated hyperexcitability, likely induced by upstream transmission from primary afferents. However, muscle fibrillation potentials seem unaffected by pharmacological perturbation. Unilateral neurectomy of the sciatic nerve, which is equivalent to disrupting muscle afferents, potentially salvages motor neurons via VGluT1 reduction in synapses at the grey matter. Whether the spontaneous neurogenic EMG activities would be affected in such cases remains to be further analyzed, though it is established that VGluT expression level does not impact disease onset and animal survival. Further, our evaluations indicate that excitotoxicity through external (presynaptic) neurotransmitter input via increased glutamate loading, and local changes (postsynaptic) via elevated surface trafficking of GluR2-less AMPA receptors, was likely an effect that ultimately affects alpha motor neuron survival. Overall, it is worth exploring the underlying mechanism within primary afferents that drives excitotoxicity.

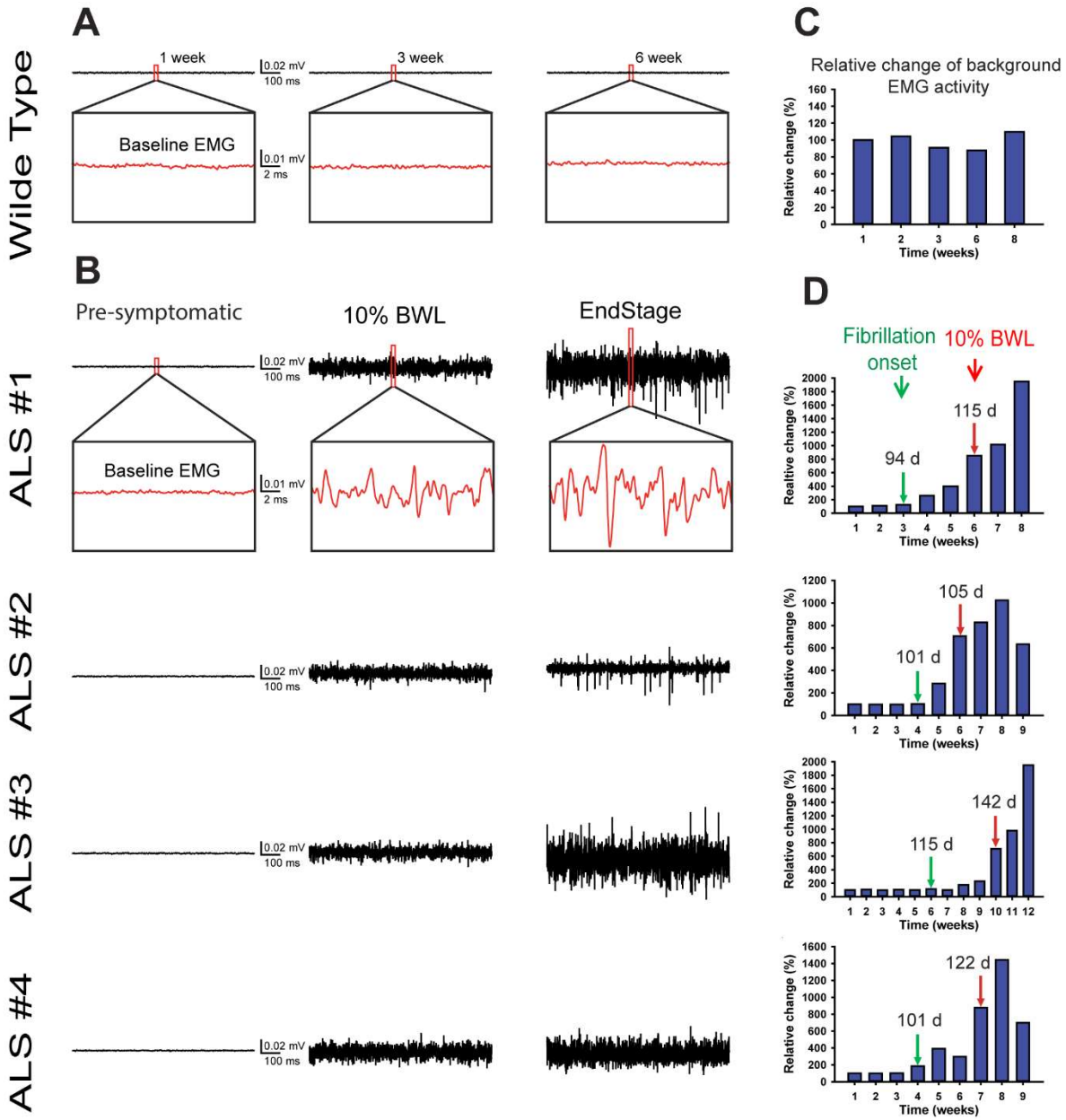

Figure 1. Time-course delineation of fibrillation potential developments in wild type and SOD1^{G93A} rats. A) Electromyographic (EMG) recordings of wild type (control) rats done at weeks 1, 3 and 6 (after animals reached 60d of age) demonstrated no visible changes. B) EMG recordings of 4 SOD1^{G93A} rats showed enhanced fibrillation potentials starting at 10% body weight loss (BWL). C) EMG recordings done up to 8 weeks in wild type rats were normalized against the activity recorded in week 1; no significant relative changes were noted. D) Relative changes in EMG recording in SOD1^{G93A} rats showed the onset of fibrillation potentials and the progressive rise of the EMG amplitude until end stage was reached. Red arrows correspond to the 10% BWL stage, whereas green arrows indicate the onset of fibrillation potentials.

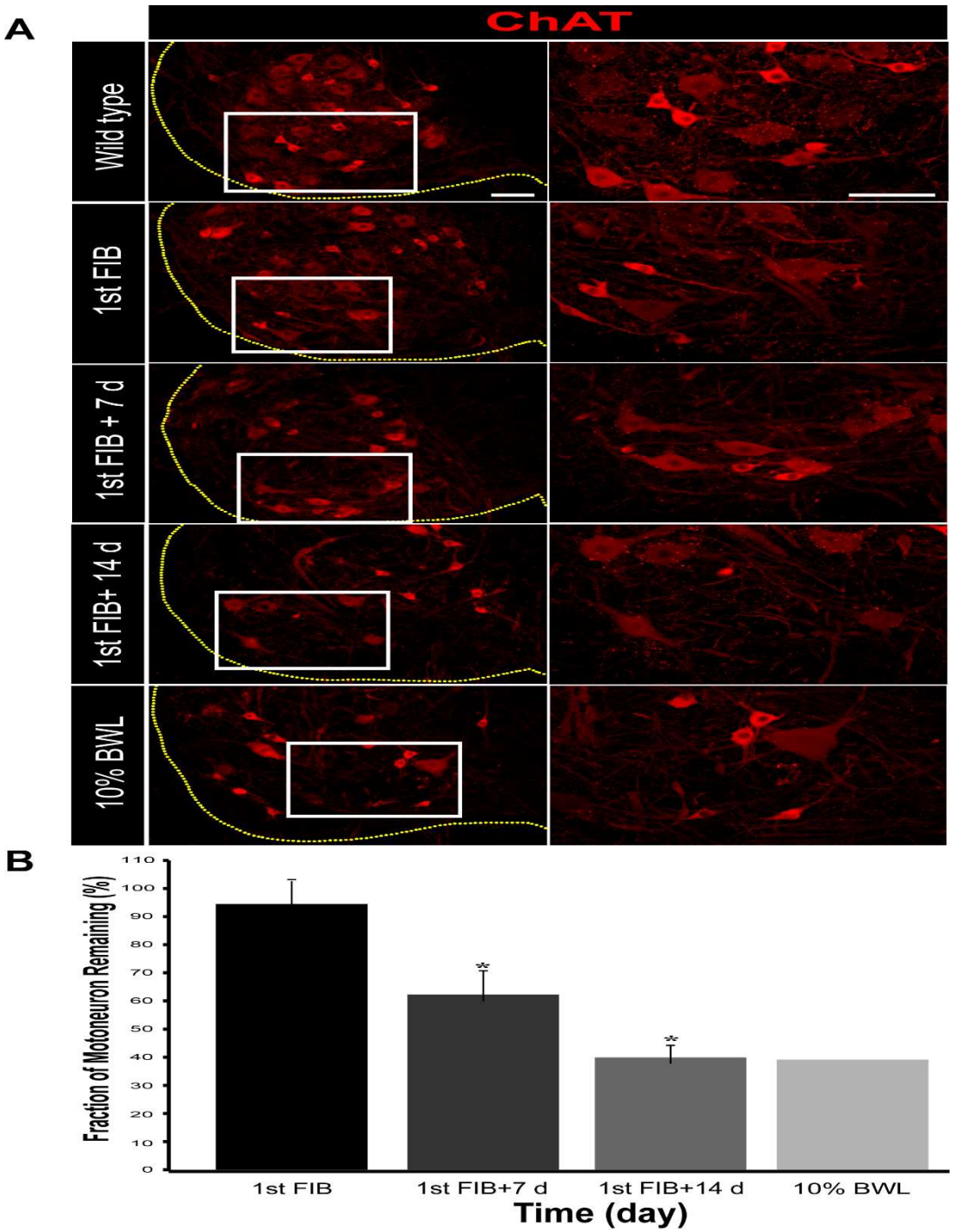

Figure 2. Time-dependent alpha motoneurons loss in L2-L6 segments in SOD1^{G93A} rats. A) 10x microscopic images (left panels) and high magnification apotome images (right panels) of spinal ventral horn show ChAT^{+} (red) staining in alpha motoneurons of both wild type and SOD1^{G93A} rats at first fibrillation (1st FIB), first fibrillation plus 7 days (1st FIB + 7 d), first fibrillation plus 14 days (1st FIB + 14 d) and SOD1^{G93A} rats with 10% of body weight loss (10% BWL). B) Normalization of alpha motoneuron count in L2-L6 lumbar segments of SOD1^{G93A} animals at different time points against the wild type animals. Data are expressed as percentages of remaining alpha motoneurons comparing to wild type animal ± SEM; $P = 0.05$. Scale bar=100 µm.

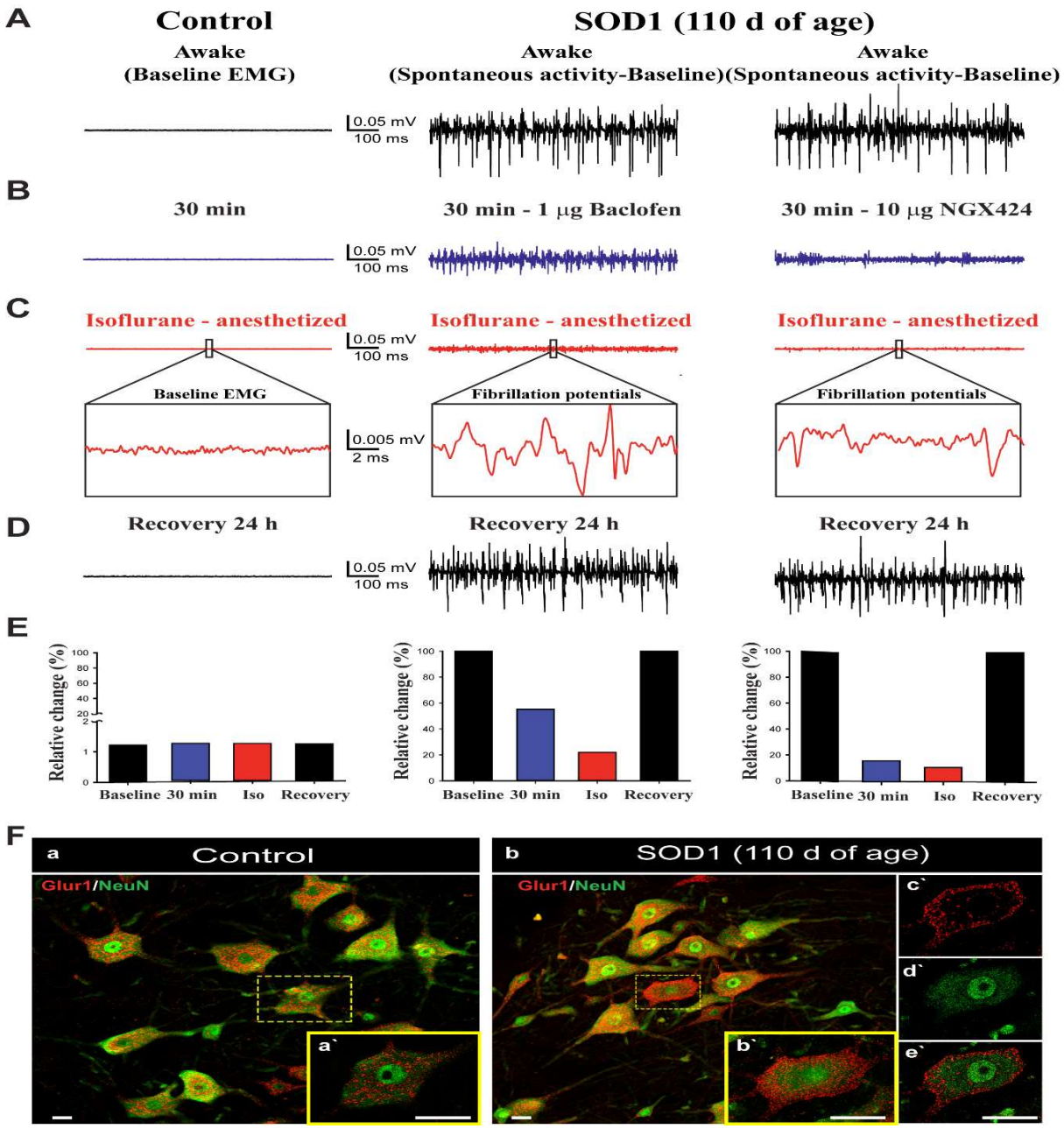

Figure 3. EMG recording capturing the presence and absence of spontaneous neurogenic activities in awake wild type and presymptomatic (age = 110d) $SOD1^{G93A}$ rats. A) Baseline EMG recording demonstrated spontaneous neurogenic activities in presymptomatic rats, but not in wild type rats. B) EMG recordings completed at 30 min after intrathecal administrations of Baclofen or NGX424 partially attenuated spontaneous neurogenic activities in transgenic rats. C) EMG recordings after 3% isofluorane administration attenuated most spontaneous neurogenic activities. The black rectangle shows an enlarged view of the fibrillation potentials that were unaffected by drug administration. D) Spontaneous neurogenic activities completely recovered 24 h after spinal drug administration. E) Comparisons between EMG recordings demonstrated in A) to D). F) High magnification apotome images (20x and 63x) of the ventral spinal cord of control (a and a') and $SOD1^{G93A}$ (b and b') rats show $GluR1^{+}$ (red) and $NeuN^{+}$ (green) staining in motoneurons. A 63x apotome optical section features the $GluR1^{+}$ (c') immunostaining on the membrane of a $NeuN^{+}$ motoneuron (d'), in addition to their co-localization (e'). Scale bar=25 μm.

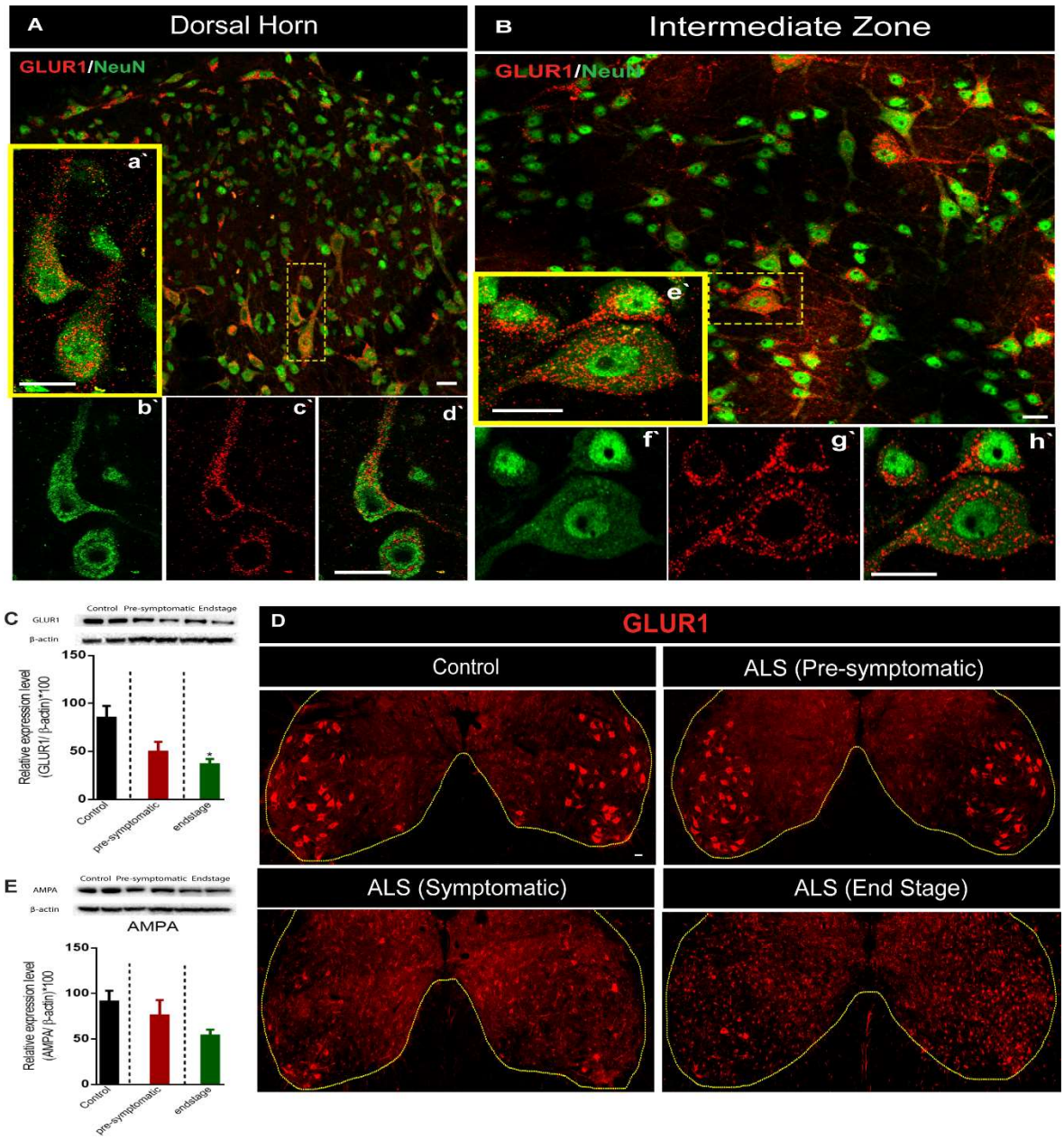

Figure 4. Downregulation of GluR1 subunit-containing AMPA receptors in the dorsal horn and intermediate zone of presymptomatic (110 d age) SOD1^{G93A} rats as ALS progressed. A) 20x and 63x (a') apotome images from the dorsal spinal cord show GluR1^{+} staining (red) and NeuN^{+} neurons (green). A 63x apotome optical section features the GluR1^{+} (b') immunostaining on the membrane of a NeuN^{+} neuron (c') and co-localization of the two (d'). B) 20x and 63x (e') apotome images from the intermediate zone of spinal cord demonstrate GluR1^{+} staining (red) and NeuN^{+} neurons (green). A 63x apotome optical section features the positive immunostaining of GLUR1 (f') on the membrane of a NeuN^{+} neuron (g') and their co-localization (h'). C) Western blot shows slight decrease in GluR1 subunit expression as ALS progressed. D) Immunofluorescence staining (10x) of GluR1 subunit in control rats and in diseased rats at different stages of ALS are shown. E) All-inclusive AMPA receptor antibodies indicate a decrease in receptor proteins as ALS progressed. Data are expressed as percentages of relative expression level ± SEM of GluR1 normalized to β-actin expression level. $P < 0.05$. The scale bar is 25 μm for high magnification images and 50 μm for 10x images.

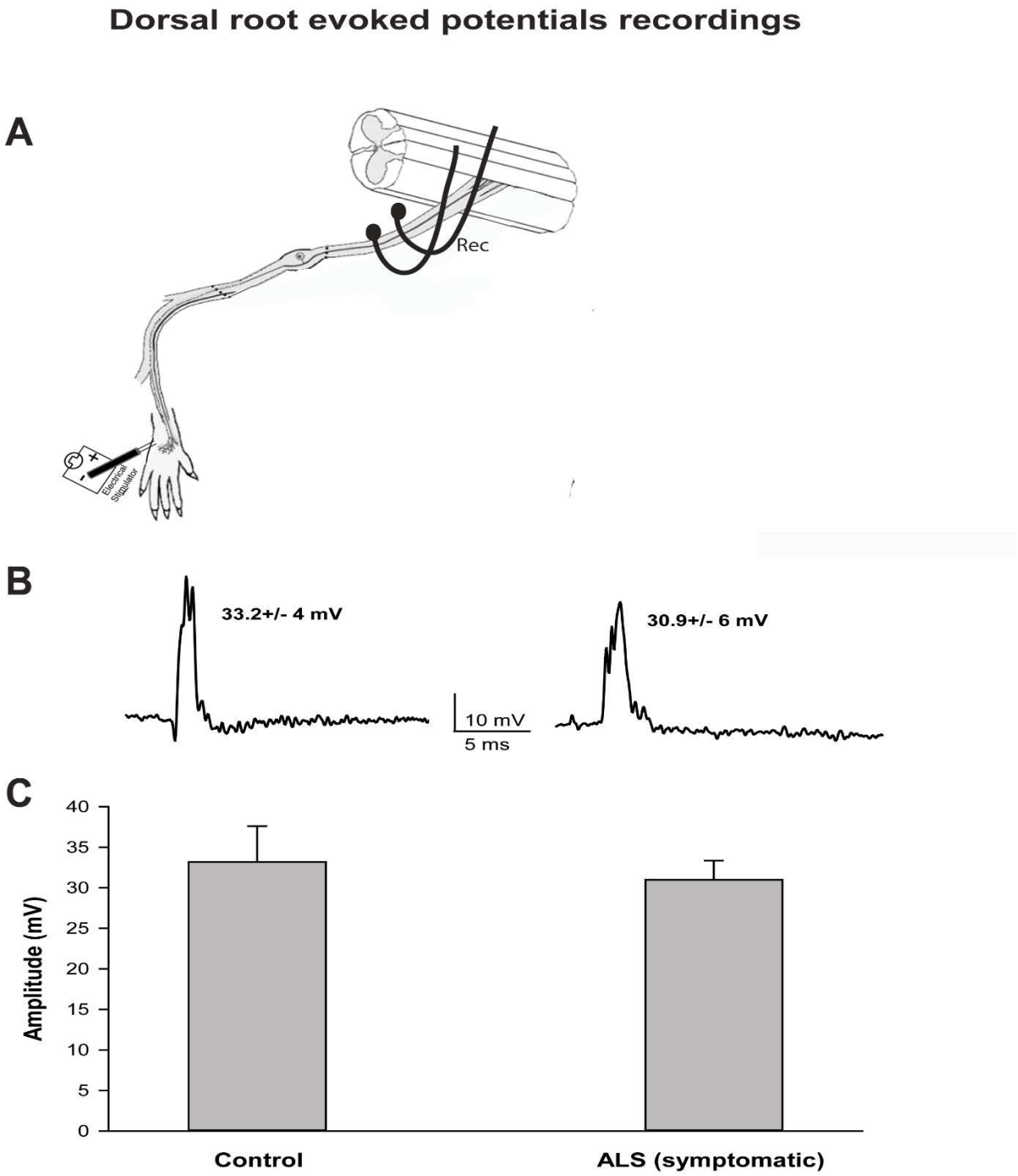

Figure 5. Dorsal root recording of primary afferent inputs in wild type and symptomatic SOD1^{G93A} rats. A) A schematic demonstration shows the lumbar spinal cord with the dorsal root attached, and lifted by two hook recording electrodes, to capture electrical signals from primary afferents. An additional pair of stimulating electrodes are placed subcutaneously in the plantar region of the animals' left paws to evoke electrical stimuli. B) Electrical responses from wild type (control, left) and symptomatic SOD1^{G93A} rats (right) are recorded in the left L5 dorsal root after an evoked electrical stimulus in the paw at the corresponding side. C) A bar graph denotes no difference in response amplitudes (mV) between wild type and symptomatic SOD1^{G93A} rats. Data are expressed as the amplitude mean in millivolts (mV) ± SEM. Student's t-test, $n \geq 3$.

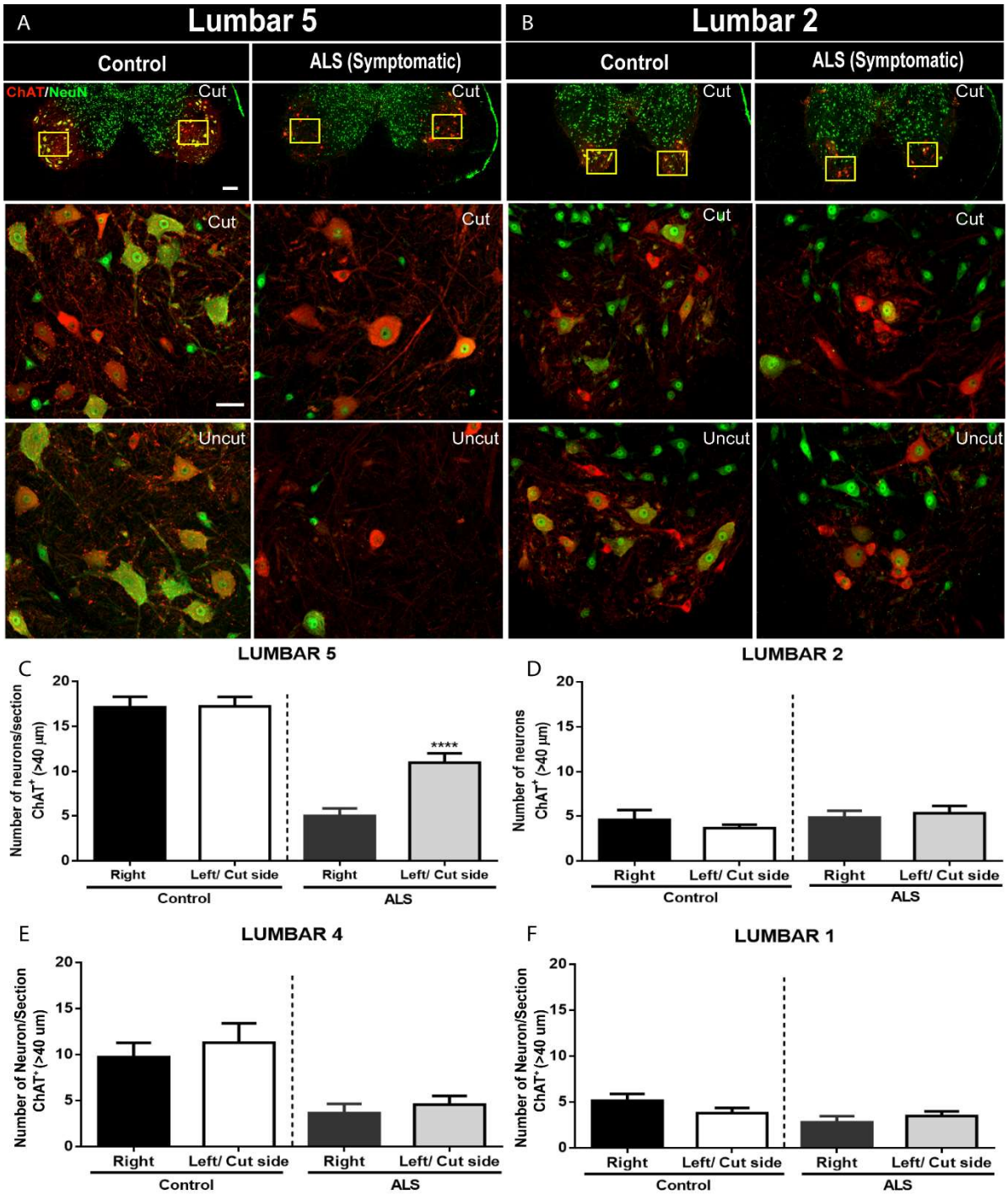

Figure 6. Alpha-motoneuron survival after unilateral sciatic neurectomy in wild type and presymptomatic SOD1^{G93A} rats. A) 10x (top panel) and high magnification apotome images (middle panel with cut nerve; lower panel with uncut nerve) of the ventral spinal cord show ChAT (red) and NeuN (Green) staining in L5 segments, and B) in L2 segments. Quantification of alpha motoneuron numbers expressed on both the left (ipsilateral to lesion site) and right (contralateral to lesion side) sides of segments C) L5, D) L2, E) L4, and F) L1. Data are expressed as number of ChAT$^+$ neurons /section ± SEM; *P= 0.0001*. The scale bar is 100 µm for 10x images and 50 µm for apotome images.

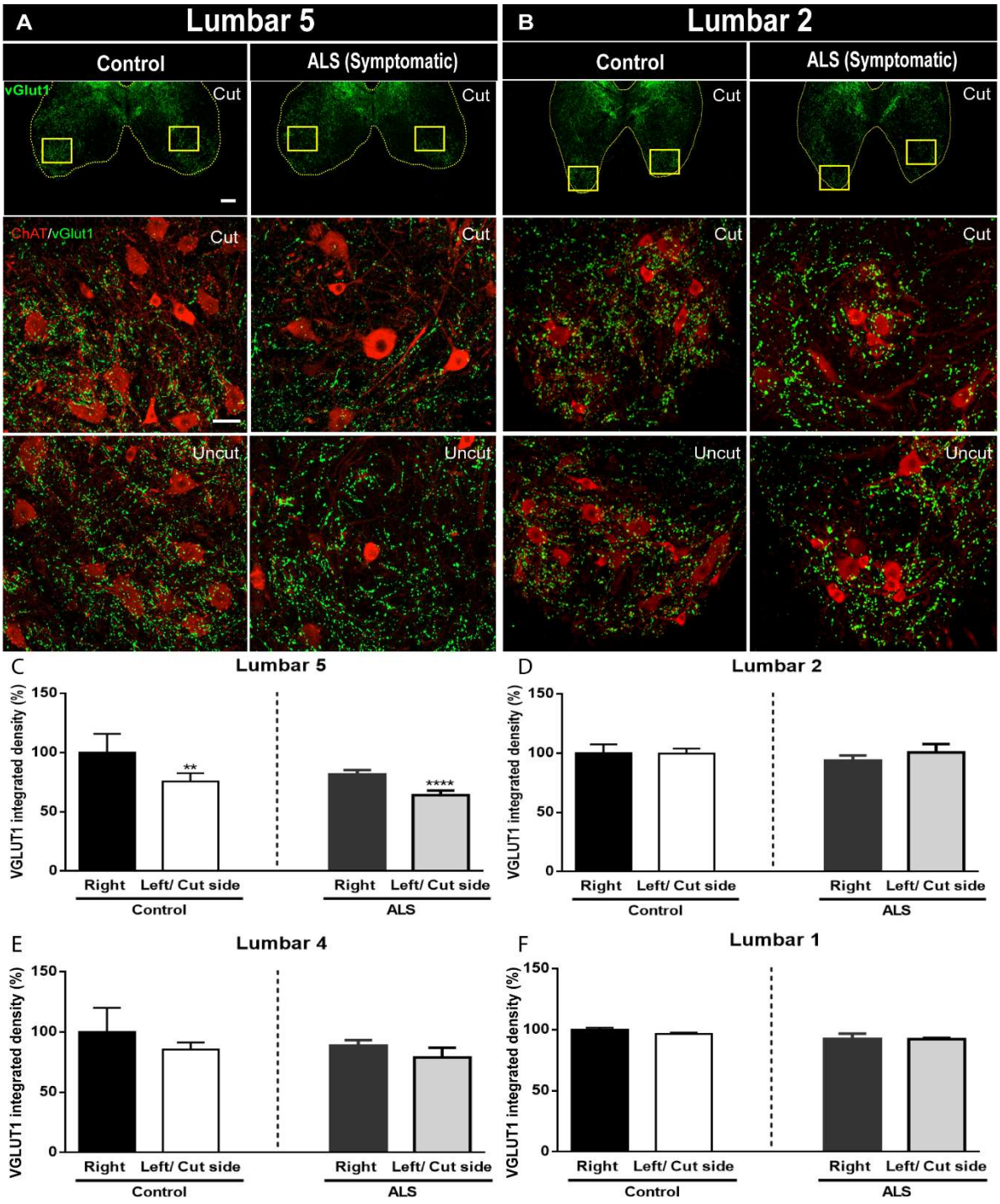

Figure 7. Immunodetection of vesicular glutamate transporter 1 (VGluT1) in wild type and SOD1^{G93A} rats after sciatic neurectomy. The 10x (top panel) and high magnification apotome images (middle panel with cut nerve; lower panel with uncut nerve) denote ChAT (red) and VGluT1 (green) immunostaining in the ventral region of A) L5 segments, and B) L2 segments. Quantification of the integrated density of VGluT1 in segments C) L5, D) L2, E) L4, and F) L1 indicated its reduced expression in L5 segments of both animal types. Data are expressed as the percentage in integrated density of VGluT1 ± SEM compared to the uncut sites of wild type rats; $P(^{**})= 0.01$ and $P(^{****})= 0.0001$. The scale bar is 100 µm for 10x images and 50 µm for apotome images.

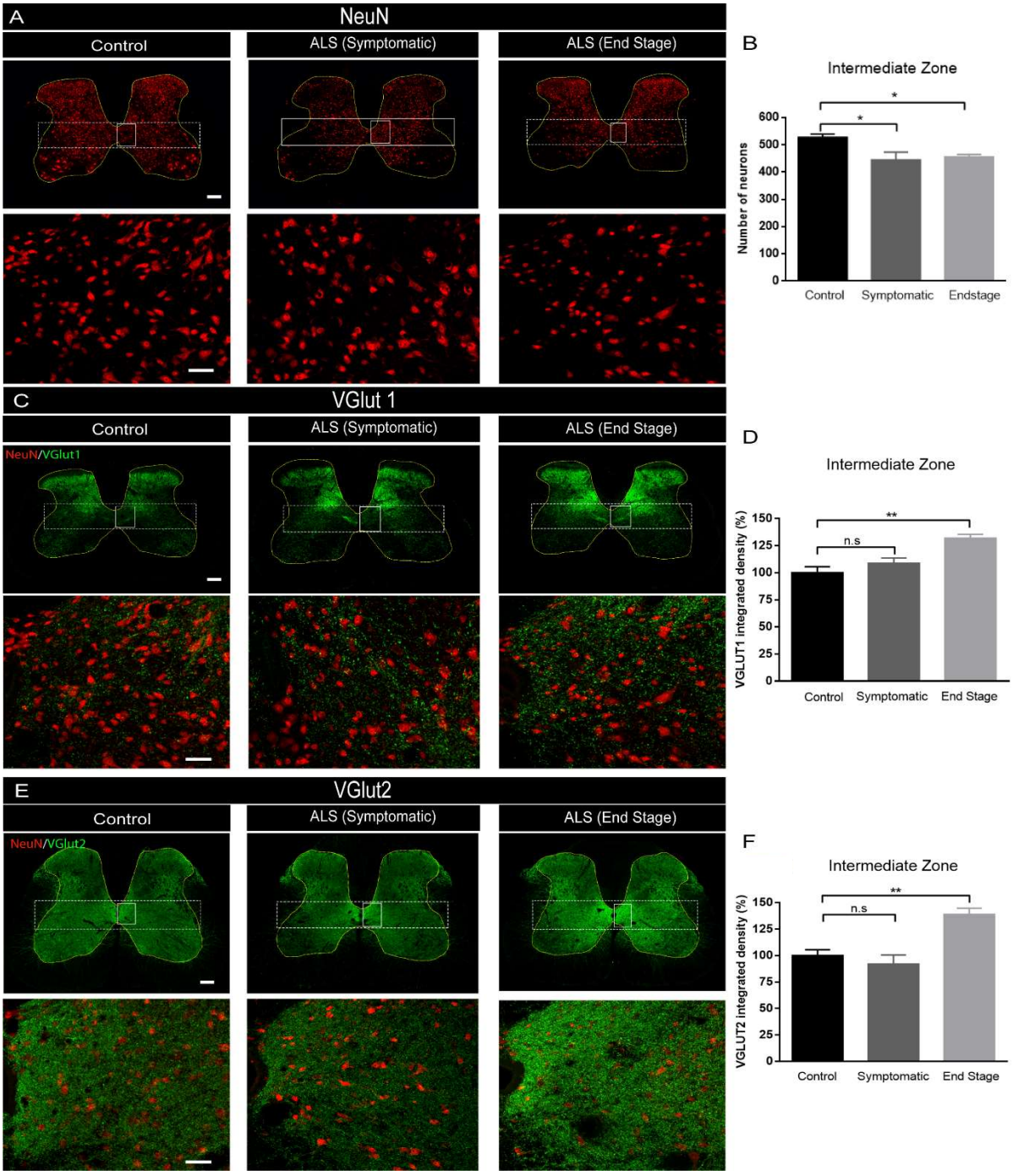

Figure 8. Expression levels of VGluT1, VGluT2 and NeuN in spinal lamina VII of wild type, symptomatic, and end-stage SOD1^{G93A} rats. The 10x (top panels of A, C, and E) and high magnification apotome images (bottom panels of A, C and E) are shown. A) & B) Quantification of interneuron count located in the intermediate zone. C) & D) Quantification of VGluT1 based on integrated density. F) Quantification of VGluT2 based on integrated density. The integrated density of VGluT1 and VGluT2 ± SEM are normalized against interneuron count; P(*)= 0.05 and P(**)= 0.001. The scale bar is 100 µm for 10x images and 50 µm for apotome images.

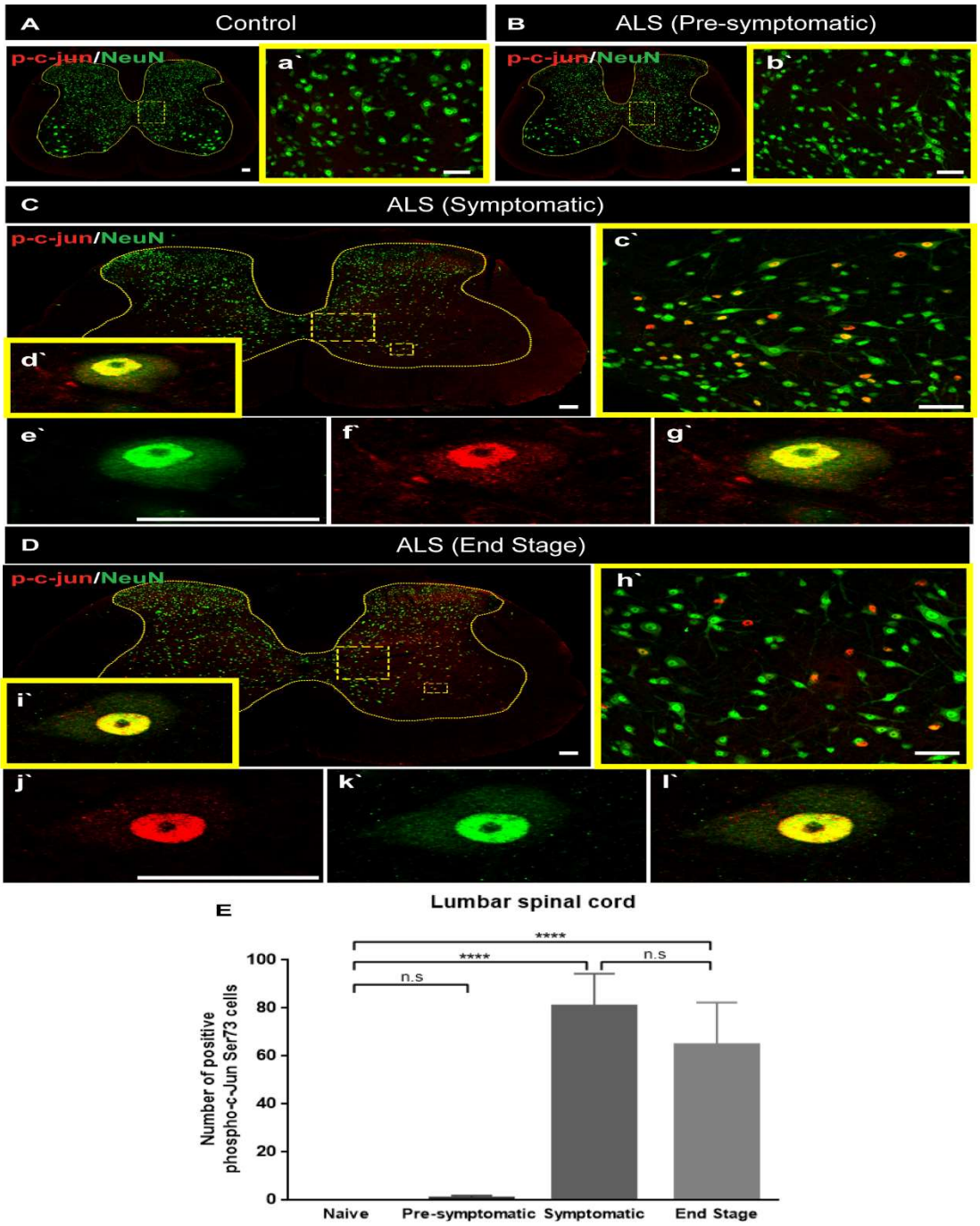

Figure 9. Expression levels of N-terminally phosphorylated c-Jun (p-c-jun) in spinal lamina VII of wild type, presymptomatic, symptomatic, and end-stage SOD1^{G93A} rats. A) & B) Minimal immunostaining for p-c-jun is detected in wild type and presymptomatic animals; such was further confirmed by the enlarged image of (a`) and (b`). C) Evident appearance of p-c-jun staining is detected in symptomatic animals, where enlarged images (c`-g`) demonstrated co-localization with NeuN staining. Similarly, D) demonstrated increased overlaps between p-c-jun staining with NeuN staining, indicating that cellular damages are taking place inside neurons (i`-l`). E) depicts the number of neurons positively stained with p-c-jun over the course of ALS development. *P(****)= 0.0001.* The scale bars are 50 µm for 10x and apotome images.

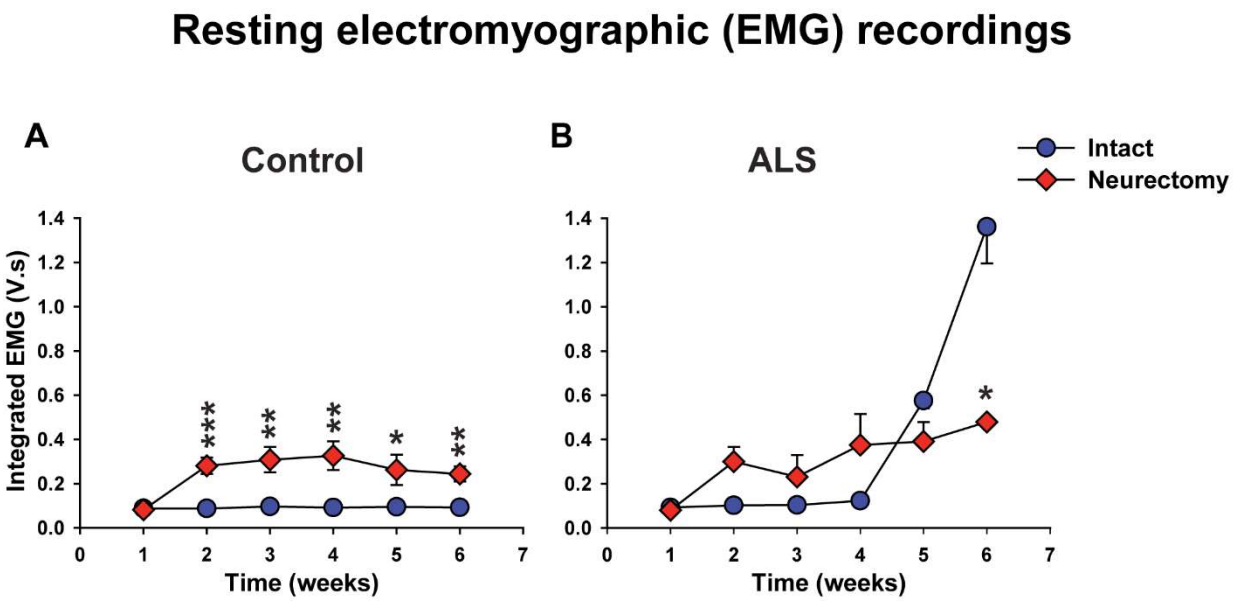

Supplementary Figure 1. Time-course delineation of fibrillation potentials recorded in anesthetized wild type and presymptomatic SOD1^{G93A} rats after sciatic neurectomy. A) Five weeks of the integrated EMG responses were obtained on the transected side (red squares) and the contralateral side (blue circles) of animals. These animals were followed until 10-20% BWL. Data are expressed as the mean of integrated EMG responses (V·sec) ± SEM; P(*) ≥ 0.05 by two-way ANOVA. It is followed by Bonferrioni post hoc test; n=3.

REFERENCES

1. Bosco, D. A., Morfini, G., Karabacak, N. M., Song, Y., Gros-Louis, F., Pasinelli, P., Goolsby, H., Fontaine, B.A., Lemay, N., McKenna-Yasek, D., Frosch, M.P., Agar, J.N., Julien, J., Brady, S.T., & Brown, R. H. (2010). Wild-type and mutant SOD1 share an aberrant conformation and a common pathogenic pathway in ALS. *Nature Neuroscience*, *13*(11), 1396-1403. doi:10.1038/nn.2660

2. Brooks, B. R. (1994). El escorial World Federation of Neurology criteria for the diagnosis of amyotrophic lateral sclerosis. *Journal of the Neurological Sciences,124*, 96-107. doi:10.1016/0022-510x(94)90191-0

3. Brown, R., Dissanayake, K. N., Skehel, P. A., & Ribchester, R. R. (2014). Endomicroscopy and electromyography of neuromuscular junctions in situ. *Annals of Clinical and Translational Neurology,1*(11), 867-883. doi:10.1002/acn3.124

4. Brumovsky, P. R. (2013). VGLUTs in Peripheral Neurons and the Spinal Cord: Time for a Review. *ISRN Neurology,2013*, 1-28. doi:10.1155/2013/829753

5. Brumovsky, P., Watanabe, M., & Hökfelt, T. (2007). Expression of the vesicular glutamate transporters-1 and -2 in adult mouse dorsal root ganglia and spinal cord and their regulation by nerve injury. *Neuroscience,147*(2), 469-490. doi:10.1016/j.neuroscience.2007.02.068

6. Ciryam, P., Lambert-Smith, I. A., Bean, D. M., Freer, R., Cid, F., Tartaglia, G. G., Saunders, D.N., Wilson, M.R., Oliver, S.G., Morimoto, R.I., Dobson, C.M., Vendruscolo, M., Favrin, G., & Yerbury, J. J. (2017). Spinal motor neuron protein supersaturation patterns are associated with inclusion body formation in ALS. *Proceedings of the National Academy of Sciences,114*(20). doi:10.1073/pnas.1613854114

7. Daube, J. R. (2000). Electrodiagnostic studies in amyotrophic lateral sclerosis and other motor neuron disorders. *Muscle & Nerve,23*(10), 1488-1502. doi:10.1002/1097-4598(200010)23:103.0.co;2-e

8. Davidson, Y. S., Raby, S., Foulds, P. G., Robinson, A., Thompson, J. C., Sikkink, S., Yusuf, I., Amin, H., DuPlessis, D., Troakes, C., Al-Sarraj, S., Sloan, C., Esiri, M.M., Prasher, V.P., Allsop, D., Neary, D., Pickering-Brown, S.M., Snowden, J.S., & Mann, D. M. (2011). TDP-43 pathological changes in early onset familial and sporadic Alzheimer's disease, late onset Alzheimer's disease and Down's Syndrome: Association with age, hippocampal sclerosis and clinical phenotype. *Acta Neuropathologica,122*(6), 703-713. doi:10.1007/s00401-011-0879-y

9. Devor, M., Govrin-Lippmann, R., & Angelides, K. (1993). Na channel immunolocalization in peripheral mammalian axons and changes following nerve injury and neuroma formation. *The Journal of Neuroscience,13*(5), 1976-1992. doi:10.1523/jneurosci.13-05-01976.1993

10. Forsberg, K., Jonsson, P. A., Andersen, P. M., Bergemalm, D., Graffmo, K. S., Hultdin, M., Jacobsson, J., Rosquist, R., Marklund, S.L., & Brännström, T. (2010). Novel Antibodies Reveal Inclusions Containing Non-Native SOD1 in Sporadic ALS Patients. *PLoS ONE,5*(7). doi:10.1371/journal.pone.0011552

11. Gale, K., Kerasidis, H., & Wrathall, J. R. (1985). Spinal cord contusion in the rat: Behavioral analysis of functional neurologic impairment. *Experimental Neurology,88*(1), 123-134. doi:10.1016/0014-4886(85)90118-9

12. Herdegen, T., Claret, F., Kallunki, T., Martin-Villalba, A., Winter, C., Hunter, T., & Karin, M. (1998). Lasting N-Terminal Phosphorylation of c-Jun and Activation of c-Jun N-Terminal Kinases after Neuronal Injury. *The Journal of Neuroscience,18*(14), 5124-5135. doi:10.1523/jneurosci.18-14-05124.1998

13. Hossaini, M., Cano, S. C., Dis, V. V., Haasdijk, E. D., Hoogenraad, C. C., Holstege, J. C., & Jaarsma, D. (2011). Spinal Inhibitory Interneuron Pathology Follows Motor Neuron Degeneration Independent of Glial Mutant Superoxide Dismutase 1 Expression in SOD1-ALS Mice. *Journal of Neuropathology & Experimental Neurology,70*(8), 662-677. doi:10.1097/nen.0b013e31822581ac

14. Howland, D. S., Liu, J., She, Y., Goad, B., Maragakis, N. J., Kim, B., Erickson, J., Kulik, J., DeVito, L., Psaltis, G., DeGennaro, L.J., Cleveland, D.W., & Rothstein, J. D. (2002). Focal loss of the glutamate transporter EAAT2 in a transgenic rat model of SOD1 mutant-mediated amyotrophic lateral sclerosis (ALS). *Proceedings of the National Academy of Sciences,99*(3), 1604-1609. doi:10.1073/pnas.032539299

15. Huang, C., Zhou, H., Tong, J., Chen, H., Liu, Y., Wang, D., Wei, X., & Xia, X. (2011). FUS Transgenic Rats Develop the Phenotypes of Amyotrophic Lateral Sclerosis and Frontotemporal Lobar Degeneration. *PLoS Genetics,7*(3). doi:10.1371/journal.pgen.1002011

16. Hughes, D. I., Polgár, E., Shehab, S. A., & Todd, A. J. (2004). Peripheral axotomy induces depletion of the vesicular glutamate transporter VGLUT1 in central terminals of myelinated afferent fibres in the rat spinal cord. *Brain Research,1017*(1-2), 69-76. doi:10.1016/j.brainres.2004.05.054

17. Isaac, J. T., Ashby, M. C., & Mcbain, C. J. (2007). The Role of the GluR2 Subunit in AMPA Receptor Function and Synaptic Plasticity. *Neuron,54*(6), 859-871. doi:10.1016/j.neuron.2007.06.001

18. Jiang, M., Schuster, J. E., Fu, R., Siddique, T., & Heckman, C. J. (2009). Progressive Changes in Synaptic Inputs to Motoneurons in Adult Sacral Spinal Cord of a Mouse Model of Amyotrophic Lateral Sclerosis. *Journal of Neuroscience,29*(48), 15031-15038. doi:10.1523/jneurosci.0574-09.2009

19. Leigh, P. N., Whitwell, H., Garofalo, O., Buller, J., Swash, M., Martin, J.E., Gallo, J.M., Weller, R.O., & Anderton, B.H. (1991). Ubiquitin-Immunoreactive Intraneuronal

Inclusions In Amyotrophic Lateral Sclerosis. *Brain*, *114*(2), 775-788. doi:10.1093/brain/114.2.775

20. Liu, X., Eschenfelder, S., Blenk, K., Jänig, W., & Häbler, H. (2000). Spontaneous activity of axotomized afferent neurons after L5 spinal nerve injury in rats. *Pain,84*(2), 309-318. doi:10.1016/s0304-3959(99)00211-0

21. Liu, Y., Beyer, A., & Aebersold, R. (2016). On the Dependency of Cellular Protein Levels on mRNA Abundance. *Cell,165*(3), 535-550. doi:10.1016/j.cell.2016.03.014

22. Ludolph, A., Drory, V., Hardiman, O., Nakano, I., Ravits, J., Robberecht, W., & Shefner, J. (2015). A revision of the El Escorial criteria - 2015. *Amyotrophic Lateral Sclerosis and Frontotemporal Degeneration,16*(5-6), 291-292. doi:10.3109/21678421.2015.1049183

23. Mackenzie, I. R., Rademakers, R., & Neumann, M. (2010). TDP-43 and FUS in amyotrophic lateral sclerosis and frontotemporal dementia. *The Lancet Neurology,9*(10), 995-1007. doi:10.1016/s1474-4422(10)70195-2

24. Matsumoto, A., Okada, Y., Nakamichi, M., Nakamura, M., Toyama, Y., Sobue, G., Nagai, M., Aoki, M., Itoyama, Y., & Okano, H. (2006). Disease progression of human SOD1 (G93A) transgenic ALS model rats. *Journal of Neuroscience Research,83*(1), 119-133. doi:10.1002/jnr.20708

25. McCluskey, L., & Falcone, D. (2018). Familial Amyotrophic Lateral Sclerosis. UpToDate. Retrieved October 26, 2018, from https://www.uptodate.com/contents/familial-amyotrophic-lateral-sclerosis.

26. Mcgown, A., Mcdearmid, J. R., Panagiotaki, N., Tong, H., Mashhadi, S. A., Redhead, N., Lyon, A.N., Beattie, C.E., Shaw, P.J., & Ramesh, T. M. (2012). Early interneuron dysfunction in ALS: Insights from a mutantsod1zebrafish model. *Annals of Neurology,73*(2), 246-258. doi:10.1002/ana.23780

27. Nagai, M., Aoki, M., Miyoshi, I., Kato, M., Pasinelli, P., Kasai, N., Brown, R.H. Jr., & Itoyama, Y. (2001). Rats Expressing Human Cytosolic Copper–Zinc Superoxide Dismutase Transgenes with Amyotrophic Lateral Sclerosis: Associated Mutations Develop Motor Neuron Disease. *The Journal of Neuroscience,21*(23), 9246-9254. doi:10.1523/jneurosci.21-23-09246.2001

28. Neumann, M, Sampathu, DM, Kwong, LK, Truax, AC, Micsenyi, MC, Chou, TT, Bruce, J, Schuck, T, Grossman, M, Clark, CM, McCluskey, LF, Miller ,BL, Masliah, E, Mackenzie, IR, Feldman, H, Feiden, W, Kretzschmar, HA, Trojanowski, JQ, & Lee, VMY. (2006) Ubiquitinated TDP-43 in frontotemporal lobar degeneration and amyotrophic lateral sclerosis. *Jounal of Cell Science*, *314*, 130–133.

29. Rock, K. L., & Kono, H. (2008). The Inflammatory Response to Cell Death. *Annual Review of Pathology,3*, 99-126. doi:10.1146/annurev.pathmechdis.3.121806.151456

30. Ross, C. A., & Poirier, M. A. (2004). Protein aggregation and neurodegenerative disease. *Nature Medicine*, *10*(7). doi:10.1038/nm1066

31. Sattler, R., & Tymianski, M. (2001). Molecular Mechanisms of Glutamate Receptor-Mediated Excitotoxic Neuronal Cell Death. *Molecular Neurobiology,24*(1-3), 107-130. doi:10.1385/mn:24:1-3:107

32. Schwab, C., Arai, T., Hasegawa, M., Yu, S., & Mcgeer, P. L. (2008). Colocalization of Transactivation-Responsive DNA-Binding Protein 43 and Huntingtin in Inclusions of Huntington Disease. *Journal of Neuropathology & Experimental Neurology,67*(12), 1159-1165. doi:10.1097/nen.0b013e31818e8951

33. Study, R. E., & Kral, M. G. (1996). Spontaneous action potential activity in isolated dorsal root ganglion neurons from rats with a painful neuropathy. *Pain,65*(2), 235-242. doi:10.1016/0304-3959(95)00216-2

34. Thonhoff, J. R., Jordan, P. M., Karam, J. R., Bassett, B. L., & Wu, P. (2007). Identification of early disease progression in an ALS rat model. *Neuroscience Letters,415*(3), 264-268. doi:10.1016/j.neulet.2007.01.028

35. Todd, A. J. (2002). Anatomy of Primary Afferents and Projection Neurones in the Rat Spinal Dorsal Horn with Particular Emphasis on Substance P and the Neurokinin 1 Receptor. *Experimental Physiology,87*(2), 245-249. doi:10.1113/eph8702351

36. Tortarolo, M., Grignaschi, G., Calvaresi, N., Zennaro, E., Spaltro, G., Colovic, M., Fracasso, C., Guiso, G., Elger, B., Schneider, H., Caccia, S., & Bendotti, C. (2006). Glutamate AMPA receptors change in motor neurons of SOD1G93A transgenic mice and their inhibition by a noncompetitive antagonist ameliorates the progression of amytrophic lateral sclerosis-like disease. *Journal of Neuroscience Research,83*(1), 134-146. doi:10.1002/jnr.20715

37. Van Den Bosch, L., Van Damme, P., Bogaert, E., & Robberecht, W. (2006). The role of excitotoxicity in the pathogenesis of amyotrophic lateral sclerosis. *Biochimica Et Biophysica Acta,*1068-1082. doi:10.1016/j.bbadis.2006.05.002

38. Virgo, L., Samarasinghe, S., & Belleroche, J. D. (1996). Analysis of AMPA receptor subunit mRNA expression in control and ALS spinal cord. *NeuroReport,7*(15), 2507-2512. doi:10.1097/00001756-199611040-00021

39. Waxman, S. G., Kocsis, J. D., & Black, J. A. (1994). Type III sodium channel mRNA is expressed in embryonic but not adult spinal sensory neurons, and is reexpressed following axotomy. *Journal of Neurophysiology,72*(1), 466-470. doi:10.1152/jn.1994.72.1.466

40. Wojcik, S. M., Rhee, J. S., Herzog, E., Sigler, A., Jahn, R., Takamori, S., Brose, N., & Rosenmund, C. (2004). An essential role for vesicular glutamate transporter 1 (VGLUT1)

in postnatal development and control of quantal size. *Proceedings of the National Academy of Sciences,101*(18), 7158-7163. doi:10.1073/pnas.0401764101

41. Xie, W., Strong, J. A., Meij, J. T., Zhang, J., & Yu, L. (2005). Neuropathic pain: Early spontaneous afferent activity is the trigger. *Pain,116*(3), 243-256. doi:10.1016/j.pain.2005.04.017

42. Xie, Y., Xiao, W., & Li, H. (1993). The Relationship between New Ion Channels and Ectopic Discharges from a Region of Nerve Injury. *Science in China (Series B),36*, 68-74. Retrieved October 26, 2018, from https://europepmc.org/abstract/med/7684918.

43. Yaksh, T. L., & Rudy, T. A. (1976). Chronic catheterization of the spinal subarachnoid space. *Physiology & Behavior,17*(6), 1031-1036. doi:10.1016/0031-9384(76)90029-9

44. Zeineddine, R., Farrawell, N. E., Lambert-Smith, I. A., & Yerbury, J. J. (2017). Addition of exogenous SOD1 aggregates causes TDP-43 mislocalisation and aggregation. *Cell Stress and Chaperones*, *22*(6), 893-902. doi:10.1007/s12192-017-0804-y